Partitition of The Excitation Energy Between The Fission Fragments in Spontaneous Fission of ^{252}Cf

M.Sc. Thesis

In

Physics engineering

University of Gaziantep

Supervisors

Assist. Prof. Dr. Hümbet AHMEDOV

Prof. Dr. Ramazan KOÇ
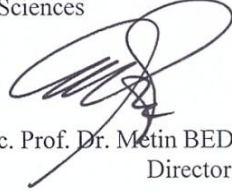
By

Mohamad KOURMO

JULY 2013

REPUBLIC OF TURKEY

UNIVERSITY OF GAZİANTEP

GRADUATE SCHOOL OF NATURAL & APPLIED SCIENCES

NAME OF THE DEPARTMENT

Name of the thesis: Partitation of The Excitation Energy Between the Fission Fragments in Spontaneous Fission of ^{252}Cf

Name of the student: MOHAMAD KOURMO

Exam date:08.07.2013

Approval of the Graduate School of Natural and Applied Sciences

Assoc. Prof. Dr. Metin BEDİR
Director

I certify that this thesis satisfies all the requirements as a thesis for the degree of Master of Science.

Prof. Dr. A. Necmeddin YAZICI
Head of Department

This is to certify that we have read this thesis and that in our consensus/majority opinion it is fully adequate, in scope and quality, as a thesis for the degree of Master of Science/Doctor of Philosophy.

Prof. Dr. Ramazan KOÇ
Co-Supervisor

Assist. Prof. Dr. Hümbet AHMEDOV
Supervisor

Assist. Prof. Dr. Hümbet AHMEDOV

Assoc. Prof. Dr. Okan ÖZER

Assist. Prof. Dr. Eser ÖZKEKLİKÇİ

I hereby declare that all information in this document has been obtained and presented in accordance with academic rules and ethical conduct. I also declare that, as required by these rules and conduct, I have fully cited and referenced all material and results that are not original to this work.

Mohamad KOURMO

ABSTRACT

PARTITITION OF THE EXCITATION ENERGY BETWEEN THE FISSION FRAGMENTS IN SPONTANEOUS FISSION OF ^{252}CF

Mohamad KOURMO

M.Sc. in Physics Eng.
Supervisors: Yrd.Doç.Dr.Hümbet AHMEDOV, Prof.Dr.Ramazan KOÇ
July 2013
88 Pages

In this thesis experimental data on mass distribution of fission fragments, kinetic energy distribution of fission fragments, neutron average multiplicity distribution of fission fragments, and neutron average emission energy from fission fragments in spontaneous fission of ^{252}Cf are analyzed in order to calculate correlation in neutron average number distribution and correlation in fission fragment average excitation energy distribution. To fulfill this task the most probable charge values for complementary light and heavy fragments in spontaneous fission of ^{252}Cf, neutron binding energy of fission fragments and the average gamma ray energy from fission fragments are estimated. The average fission fragment excitation energy then is estimated. Results of calculations are in satisfactory agreement with the corresponding experimental results.

Key words : Nuclear Fission, ^{252}Cf , Neutron number, Excitation Energy, Correlation

ÖZET

FISYONDA UYARILMA ENERJISININ TAMAMLAYICI PARÇALAR ARASINDA PAYLAŞIMI(^{252}CF SF)

Mohamad KOURMO

Yüksek Lisans Tezi, Fizik Müh. Bölümü

Tez Yöneticisi(leri): Yrd.Doç.Dr.Hümbet AHMEDOV, Prof.Dr.Ramazan KOÇ

Temmuz 2013

88 sayfa

Tez'de ^{252}Cf çekirdeğinin kendiliğinden(spontane) bölünmesi zamanı uyarılma enerjisinin bölünmüş parçalar (fisyon ürünleri) arasında paylaşımı hesaplamaları yapılmıştır. Bu amaçla füzyon parçalarının kütle ve kinetik enerji dağılımları, açığa çıkan nötron sayısı ve ortalama nötron enerjisi için deneysel veriler incelenmiş, füzyon ürünlerinin en ihtimalli elektrik yük değerleri ve onlardan açığa çıkan nötronların bağlanma enerjileri hesaplanmıştır. Fisyon ürünlerinden açığa çıkan gamma parçacıklarının enerji değerleri hesaplandıktan sonra uyarılma enerjileri değerlendirilmiş ve bu enerjinin dağılımındaki korelasyon(bağlılaşım) katsayısı ve uyarılma enerjisi paylaşımını tanımlayan diğer parametreler hesaplanmıştır. Elde edilen sonuçların benzer deneysel sonuçlarla uyum içinde olduğu sonucuna varılmıştır.

Anahtar Kelimeler: Nükleer Fizyon, ^{252}Cf, Nötron sayısı, Uyarılma Enerjisi, Korelasyon

To the heart and pulse

To the body and soul

To my parents, God saved

ACKNOWLEDGEMENTS

TABLE OF CONTENTS

LIST OF TABLES

LIST OF FIGURES

CHAPTER 1

INTRODUCTION

In 1934, Fermi and co-workers investigated thorium and uranium by neutron bombardment and as a result of their experiments it was suggested that beta radioactive elements are observed [1]. In fact, in this experiment the fission fenomena was firstly obsorved but not recognised.

Later, O.Hehn, L. Meitner, and F.Stressmann had developed neutron experiments with uranium [2-4]. In these works of the authors it was confirmed that the observed radioactive elements were lighter than those suggested, namely fission fragments which are produced in the reaction.

L. Meitner and O. R. Frish first [5] suggested the process like the splitting of liquid drop into two droplets of smaller sizes. The authors were also noted that for most heavier nuclei coulomb repulsion force compensate short range nuclear attractive force, like surface tension of droplet prevents change of nuclear shape. Therefore small energy is required for critical nuclear deformation, at the same time a gaint energy (approximatly 200 MeV) released in fission. Direct improvement of fission fenomenon for thorum and uranium was first stated by O. Frish [6]

However, it was stated by N. Bohr [7] that every nuclear reaction occuring in the result of interaction of any particle with a nucleus elepsed in two stages; first stage is the formation of highly excited compound nucleus living very short time, and second stage is the decay of compound nucleus with different open channels, neutron emission, γ- emission, and so on. For heavy nuclei the fission process competing with other process is also possible. Cross section of the nuclear reaction in the neutron induced process can be expressed as

$$\sigma\,(n,a) = \ \sigma_c \cdot G_a \qquad\qquad (1)$$

In this equation σ_c is the cross section of compounend nuclear formation and G_a is the probability of decay of component nucleus through the

channel a, where a may also indicate fission. In the fission process it is necessary some energy to be transformed into deformation energy, sufficiently high to lead fission [8].

In the work of N. Bohr and J.A. Wheeler [9] the mechanism of fission process and effects related with fission process have been studied in great details. The work is based on liquid drop model of nucleus. Nuclear critical deformation energy is considered relative to the potential energy of liquid drop of nuclear unstable equilibrium state, and critical energy is related with nuclear charge and mass number. The decay probability in this theory is dependent on parameter of critical deformation energy, and on distribution of nucleus energy levels in this state. This mechanism was later applied for spontaneous and particle induced fission for different particle kinds. This theory had great importance in further developement of fission experiments and theories.

Even Bohr – Wheeleer theory explains very useful characterictics of nuclear fission mechanism however, some questions become unclear. One of the problems is the energy balance in fission. The question is, how the total avalibale energy, i.e. the sum of energy released $\bar{Q}(A_L, A_H)$ and the excitation energy of the compound nucleus E_C in induced fission is distributed on both complementary fragments. In spontaneus fission $E_C = 0$. The kind of fragment energies are the kinetic energies $\bar{T}(A_L), \bar{T}(A_H)$, which can be measured directly, and the excitation energy $\overline{E^*}(A_L) , \overline{E^*}(A_H)$, which can be deduced from exerimental data on $\bar{v}(A)$ as well as average total γ- ray energy $\overline{E_\gamma}(A)$. The Two Spheroid Model (TSM) , which has been described in Refs[10,11], is a simple scission point model based on a general energy balance :

$$\bar{Q}(A_L, A_H) + E_c = \overline{TKE}\ (A_L, A_H) + \overline{E^*}(A_L, A_H) \tag{2}$$

where $\overline{TKE}\ (A_L, A_H) = E_{pre} + E_{coul}$, and $\overline{E^*}(A_L, A_H) = E_{def}^L + E_{def}^H + E_{dis} + E_h$,
E_{pre} - pre − scission kinetic energy, E_{coul} - coulomb potential energy at scission, E_{def}^i - deformation energy of fragment i at scission, E_{dis} - intrinsic excitation energy at scission due to dissipation between second − saddle point of fission barrier and scission point, E_h - intrinsic excitation energy (" heat ") at the second- saddle point.

$E = E_{coul} + E^L_{def} + E^H_{def}$ potential energy at scission for given mass asymmetry, E^i_{int} - intrinsic excitation energy of fragment i at scission.

According to Terrell [12] the fissioning system may be discribed as two spheroidically shaped fragments nearly touching at the scission point. The nuclear forces between the fragments cause a small distance $d \sim 1.4$ fm at the place of contact as in Ref [13].

The TSM as a scission point model with semi-empirical, temperature-dependent shell correction energies for deformed fragments at scission is successful in describing the main features of energy partition in fission as function of mass asymmetry. The diminution of shell effects due to scission point temperature, which depends on the dissipated energy as well as inciderable changes of fragment energies as function of E_c (or E_i). It is emphasized, that the average features of energy partition in fission as function of mass asymmetry are described.

In the induced fission process of heavy nuclei channel effects appearing at scission threshold are not usually taken into account. However, they could be considered approximatively by using effective values for the fission barrier and, thus, simulating collective transition states.

The results of TSM calculations are the necessary precondition for the application of complex statistical fission neutron theories for calculations of energy and angular distributions Ref [10,13].

The problem of sharing of total excitation energy of final fragments between the fragments has been discussed in Ref [14] by the condition of equal temperatures. In this study, it is also discussed the intrinsic excitation-energy partition in statistical equilibrium for different level-density descriptions as a function of the total intrinsic excitation energy of the fissioning system. Excitation energies are found to be strongly enhanced in the heavy fragment, if the level density follows a constant-temperature behavior at low energies, e.g, in the composed Gilbert-Cameron description Ref[15]. The final excitation energy in each fission fragment is built up from different contributions that arise at different steps of the fission process. Only the intrinsic excitation energy available at scission is shared between the fragments according to statistical equilibrium. The deformation and collective energies are dissipated into intrinsic excitation energy after scission, when the fragments are not in contact anymore. These two types of energies cannot be exchanged between the

fragments. The work [14] conclude that the assumption of most fission models used for the prediction of prompt neutron emission that the total excitation energy (TXE) is shared between the fragments according to the condition of the equal final temperatures is not correct.

The work [14] also investigates the intrinsic-excitation-energy partition for a specific mass split assuming two different level-density descriptions, disregarding shell effects: Energy sorting occurs for excitation energies in excess of 4 MeV if the level densities of the nascent fragments are characterized by a constant, energy-independent temperature. As a second case, a combined description with a transition from a constant-temperature regime at low excitation energies to a Fermi-gas regime at higher excitation energies has been choosen. This type of description leads to a strongly enhanced excitation energy in the heavy fragment at low energies, reaching well above the matching energies.

As it follows from discussion made above the problem of energy balance in fission or in other words the partitation of total excitation energy between the fission fragments note yet theoritically cleared out because of complicated and many functional dependence of the excitation energy partitation between the fission fragments. In this point the thermodynamic behavior of nuclear matter in scission plays definite role.

In thesis we investigate the problem of sharing of total excitation energy between the fission fragments in spontaneous fission of ^{252}Cf by use of experimental data of C.Budtz-Jorgensen and K.Knitter [16] on neutron average multiplicity dependent on fragment mass, neutron average energy dependent on fission fragment mass and fission fragment kinetic energy dependent on fragment mass. We use also mass distribution yield in spontaneous fission of ^{252}Cf of experimental work from Ref[17] and semi- emprical equation for average gamma radiation energy dependent on fission fragment mass of work [18]. Terrell approximation [19] is also used for the estimation of average gamma energy from fission fragment. We investigate firstly, the correlation between neutron multiplisities from complementary fission fragments because of it main contribution to the excitation energy and then study the correlation between excitation energies from complementary fission fragments as a measure of sharing mechanism of total excitation energy between the fission fragments in the different mass ranges of fission fragments corresponding to the different mechanism of fission process.

In Chapter 2, the mechanism of fission given by Bohr and Wheeler, formation of fission barriar in classical theory of fission as well as Shell corrections reduced to double humped fission barrier is given. The work of Wilkins [20] deduced to explain fission fragment nucleus charge, mass, and kinetic energy distributions in fission of different heavy spontaneously and induced fissioning nuclei, as well as multi-model fission model is also discussed in this chapter. Experimental results for mass distribution in spontaneous fission of ^{252}Cf and analytical approximation of mass distribution is also represented.

In Chapter 3, it is discussed the experimental data of C .Budtz-Jorgensen and K.Knitter on average total kinetic energy distribution of fission fragment for ^{252}Cf and most probable charge number is identified for the given fragment mass, then energy relase for different mass division modes in spontaneous fission of ^{252}Cf is calculated. These steps are necessary for calculating excitation energy of fission fragments.

In Chapter 4, experimental data on neutron multiplicity is analyized and correlation between neutron numbers from complementary fission fragments is calculated for the choosen mass ranges of fission fragments. This correlation is very important for understanding of excitation energy partitation between the fission fragments.

In the last Chapter the excitation energy from complementary fission fragments is calculated. For this reason, binding energy of neutrons, average gamma energy is calculated for the fission fragments. Finally, excitation energy coreelation coefficient is estimated.

In section Results, the main findings of the work is described. References are given following the chapter results. At the final pages of thesis Appendixs are given for completness and clearity of thesis.

In production of thesis "MICROSOFT OFFICE" facilities and "MATHEMATICA" program are used.

CHPTER 2

FISSION MODELS AND THE MASS DISTRIBUTION OF FISSIN FRAGMENTS

2.1. Fission barrier for fission of heavy nuclei

Simple model that represents the mechanism of nuclear fission in both, induced and spontaneous fission is the nuclear liquid drop model, which assumes the nucleus as uniformly charged, impressible liquid drop. The mechanism of nuclear fission was worked out by N.Bohr and J.A. Wheeler in 1939 [9].

2.1.1. Liquid Drop Model

To study nuclear stability respect to nuclear deformation N.Bohr and J.A. Wheeler suppose nuclear surface equation dependent on polar angle θ as

$$r\,(\theta) = \; R[1 + \alpha_0 + \; \alpha_2 P_2\,(\cos\theta) + \alpha_3 P_3\,(\cos\theta) + \; ....\,], \qquad (2.1.1)$$

where R is the initial nuclear radius, α_n are small parameters, $P_n(\cos\theta)$ are Legendre polariminals given by

$$P_n(\cos\theta) = \frac{1}{2^n \cdot n!} \cdot \frac{d^n (\cos^2\theta - 1)^n}{d\,(\cos\theta)^n} \qquad (2.1.2)$$

Weizsacker semi empirical mass equation (or for nuclear binding energy) [21,22]

$$B = [(Zm_p + Nm_n) - M_{nucl}\,(Z,N)]c^2$$

$$= a_v A - a_s A^{2/3} - a_{sym}\,(Z-N)^2 A^{-1} - a_c Z^2 A^{\frac{-1}{3}} + \delta_p\,(Z,N) \qquad (2.1.3)$$

First member is a basic part of nuclear binding energy and is called volumical part. It refers   nuclear   binding   energy   if   no   other   effects   are

existing. Second term is called surface term and is due to nuclear surface tension effect similar to surface tension energy of a liquid drop. This member reduced nuclear binding energy because of

additional energy is required to its formation. Third term is symmetry energy and is due to symmetry of protons and neutrons in nucleus. When Z=N, then it vanishes. Fourth term is the Coulomb energy arising as a result of Coulomb repulsive forces between the protons. Last term is pairing energy that is due to the odd-even nucleonic numbers determined as

$$\delta_p(Z,N) = \begin{cases} a_p A^{\frac{-1}{2}}, even-even\ nucleus \\ 0,\ even-odd\ nucleus \\ -a_p A^{\frac{-1}{2}}, odd-odd\ nucleus \end{cases}, \tag{2.1.4}$$

where a_p is a constant.

Consider nuclear fission induced by a neutron. In accordance with compound nuclear model incident neutron energy distributed over all nuclear particles being excite the nucleus. In the nuclear liquid drop it is occur vibrations and deformations of nuclear form. The volume of impressible nuclear liquid drop does not change in deformation process, and the members of the above expression, except Coulomb and surface terms don't change. Thus, in this simple approximation nuclear fissility condition depends on the change of these two terms.

 Note that more particle and good expression finding by Myers and Swiatecki [22] for nuclear binding energy has the form

$$B = [15{,}68A - 18{,}56A^{2/3} - 28{,}1\,(Z-N)^2 A^{-1}\left(1 - 1{,}18A^{-1/3}\right) - 0{,}717Z^2 A^{-1/3}\left(1 - \right.$$

$$\left. 1{,}69A^{-2/3}\right) + \delta_p(Z,N) + (nuclear\ shell\ efect)] \tag{2.1.5}$$

containing all basic properties of the above equation (2.1.1). The member $1{,}18A^{-1/3}$ is the correction to nuclear symmetry energy that is due to the surface effects, and correction $1{,}69A^{-2/3}$ is the proton – neutron exchange correction of the Coulomb energy. These corrections do not affect on the deformation energy of nucleus.

If initial nucleus is to be assumed of spherical form then its surface energy is expressed as

7

$$E_{s_0} = 4\pi R_0^2 \Omega = 4\pi \left(r_0^2 A^{2/3}\right)\Omega \tag{2.1.6}$$

where R_0 is the nuclear radius determined as $R = r_0 A^{2/3}$, Ω is the surface tension constant of a nucleus. Coulomb energy of spherical nucleus is expressed as

$$E_{c_0} = \frac{3}{5} \frac{(Ze)^2}{4\pi\varepsilon_0 R_0} \tag{2.1.7}$$

where ε_0 is the permittivity of free space. In the idealization of the nucleus the potential energy change will be associated with shape distortion terms of the interplay between surface and Coulomb effects and no account is taken of all shell effect or residual interactions arising from the independent particle motion in the nucleus.

Considering nucleus to be impressible it can be shown that the surface of the deformed nucleus having axial symmetry, is expressed as

$$S = 4\pi R_0^2 \left(1 + \frac{2}{5}\alpha_2^2\right) \tag{2.1.8}$$

Consequently, nuclear surface energy becomes

$$E_s = E_{s_0}\left(1 + \frac{2}{5}\alpha_2^2\right) \tag{2.1.9}$$

In other words, nuclear surface energy is increased due to a distortion of the form $P_2(cos\theta)$. The Coulomb energy is decreased with deformation and becomes

$$E_c = E_{C_0}\left(1 - \frac{1}{5}\alpha_2^2\right). \tag{2.1.10}$$

In order to deformed liquid drop be stable against small distortions the decrease in Coulomb energy

$$\Delta E_c = E_c - E_{C_0} = -\frac{1}{5}\alpha_2^2 E_{C_0} \tag{2.1.11}$$

must be smaller than the increase in surface energy

$$\Delta E_s = E_s - E_{s_0} = \frac{2}{5}\alpha_2^2 E_{s_0}, \tag{2.1.12}$$

the increase in surface energy corresponds to decrease of nuclear binding energy and the decrease of Coulomb energy corresponds to increase of binding energy. The drop becomes unstable if

$$x = \frac{|\Delta E_c|}{\Delta E_s} = \frac{E_{C_0}}{2E_{s_0}} \geq 1. \tag{2.1.13}$$

In this case the potential energy difference of the nucleus will be negative

$$\Delta E = \Delta E_s - |\Delta E_c| \leq 0, \tag{2.1.14}$$

While $\Delta E > 0$ or $x < 1$ the liquid drop is stable with respect to small distortions. x is called the fissility parameter. In terms of a nuclear charge and mass the surface and Coulomb energies of undistorted nucleus are expressed (in MeV) as,

$$E_{C_0} = 0,7103 \, \frac{Z^2}{A^{1/3}} (MeV), \; E_{s_0} = 17,80 A^{2/3} (MeV) \tag{2.1.15}$$

Thus, for the fissility parameter we find

$$x = \frac{Z^2}{50,13A} \tag{2.1.16}$$

The nuclear instability condition respect to the fission can be expressed as Z^2/A .

The above relation for nuclear fissility parameter and nuclear instability was given in the work Bohr and Wheeler [9].

2.1.2. Fission Barrier

The liquid drop model with only α_2 deformation would predict no barrier. Because the potential energy difference in this case is expressed as

$$\Delta E = \Delta E_s - |\Delta E_c| = \frac{2}{5}\alpha_2^2 E_{s_0} - \frac{1}{5}\alpha_2^2 E_{C_0} = \frac{\alpha_2^2}{5}\left(2E_{s_0} - E_{C_0}\right), \tag{2.1.17}$$

which is proportional to the square value of α_2. But if we take into account two symmetric deformation terms with α_2 and α_4 then one can illustrate surface, Coulomb and net deformation energies as a function of α_2 for a cut through potential

energy surface corresponding to $\frac{dE}{d\alpha_4} = 0$. In this approximation all the coefficients of deformation orders higher than α_4 are to be admitted zero. In figure below, there is a large cancellation between two contributions to the distortion energy. At the saddle ΔE_s, the increase in surface energy relative the sphere is 84.5 MeV, while ΔE_c , the decrease in Coulomb energy is 77,0 MeV. The net deformation energy is only 7,5 MeV[21].
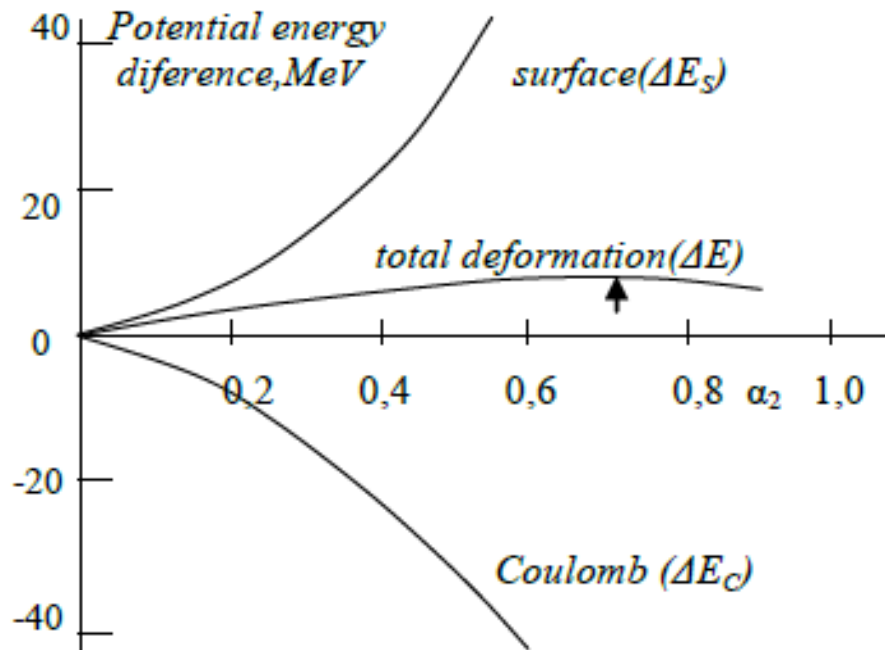
Figure 2.1. Dependences of $\Delta E_s, \Delta E_c$ and $\Delta E = \Delta E_s - |\Delta E_c|$ versus α_2 at the value of α_4 correspond to $\frac{dE}{d\alpha_4} = 0, where \Delta E = f(\alpha_2, \alpha_4)$. Surface, Coulomb and deformation energy differences for ^{252}Cf (x=0,76) versus deformation parameter α_2 [21].

A simple fission barrier is shown in Figure 2.2. Potential energy difference at the saddle (the point of maximum deformation energy) is referred as fission barrier height or activation energy and denoted as E_f.
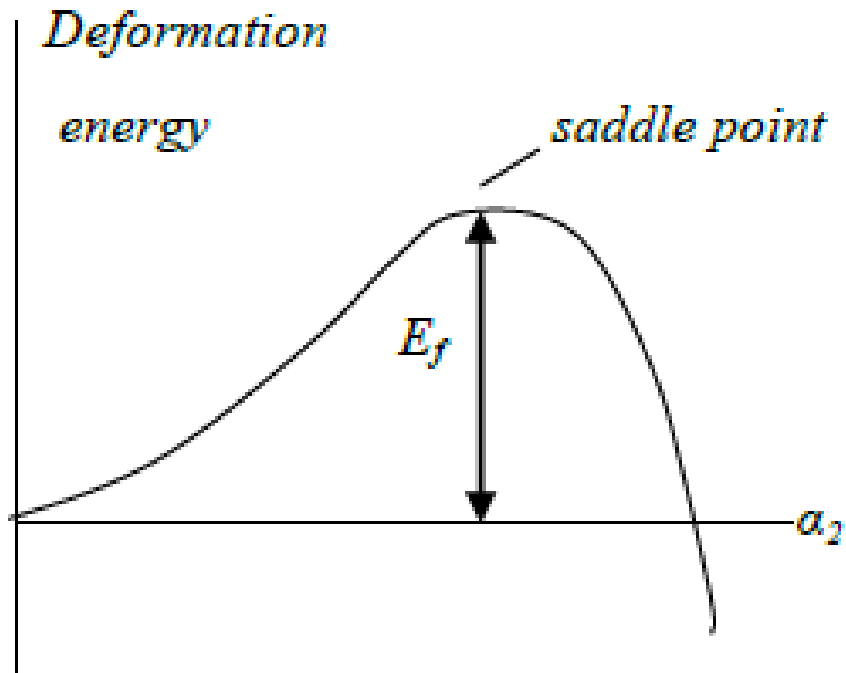
Figure 2.2. Fission barrier of a deformed nucleus. E_f is the maximum value of potential difference. Deformation corresponding to this point is referred to as critical deformation. Corresponding point on the potential energy surface is referred to as saddle point.

The shape of a nuclear surfaces corresponding to various locations on an $\alpha_2 - \alpha_4$ map is shown below. The figures possess rotational symmetry about the horizontal axis.
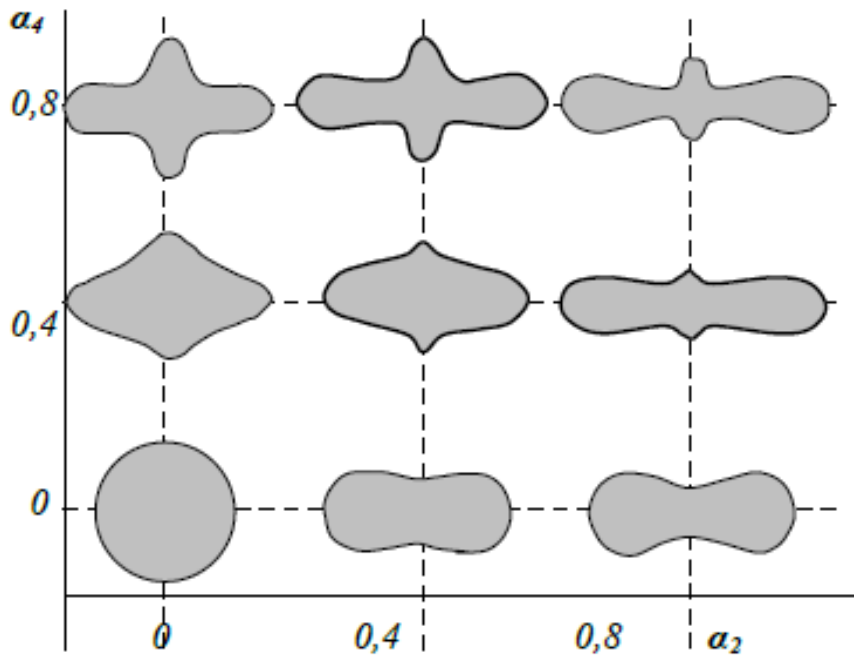
Figure 2.3. $\alpha_2 - \alpha_4$ deformation of nuclear surface. Along the vertical l dashed lines nuclear shapes are indicated for the different values of α_2. Along the horizontal dashed lines nuclear shapes are indicated for the different values of the parameter α_2 at the definite values of α_4[21].

The saddle point shapes of a nucleus in different values of x are illustrated in figure below. These forms of the nucleus are those when potential energy difference (or nuclear deformation energy) becomes maximum. As x decreases from unit down to 0.7 the saddle configuration becomes stretched to a cylindrical shape. As x decreases below 0.7, the saddle configuration develops a well defined neak and for x less than 0.6 the maximum elongation actually decreases. The transition from stretching to necking –in with decreasing x is rather sharp, accruing at $x \approx 0{,}67$.

Illustration of saddle configurations and potential energies of a deformed nucleus at different x are shown below in Figure 2.4.

Figure 2.4. a, b and c illustrate deformation configurations of fisioning nuclei at the saddle point for different values of fissility parameter x, and corresponding potential energy change of nuclei " falling " from saddle to scission.
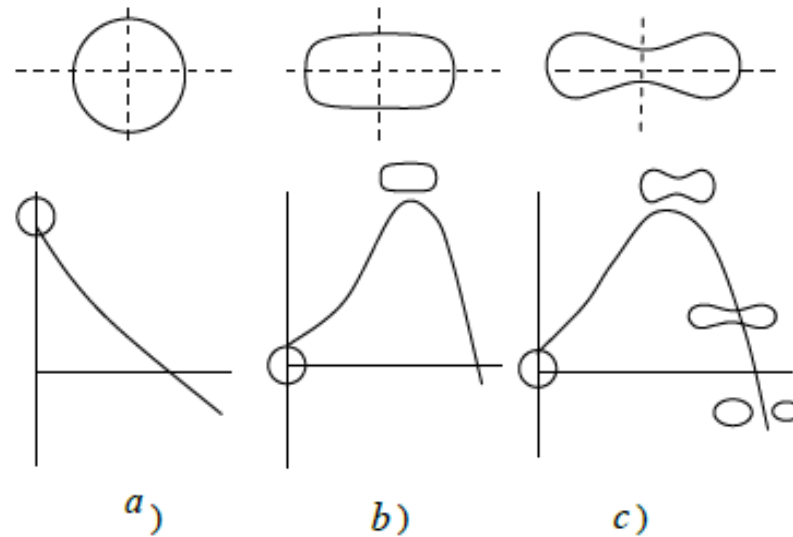
Figure 2.4. Saddle configurations and potential energies of a deformed nucleus at different x [21]. Upper figure a), b) and c) are illustrate saddle configurations corresponding to the facility parameters $x = 1$, $x = 0,8$, and $x = 0,6$, respectively. Figures just below illustrate corresponding deformation energies versus nuclear deformation. In figure c) the nuclear "falling " from saddle to scission and then to fragmentation is illustrated. At the top of each potential energy curve the nuclear saddle configurations are shown.

Calculation results for potential energy difference of a uniformly charged drop at different fissility parameter values are illustrated in the Figure 2.5
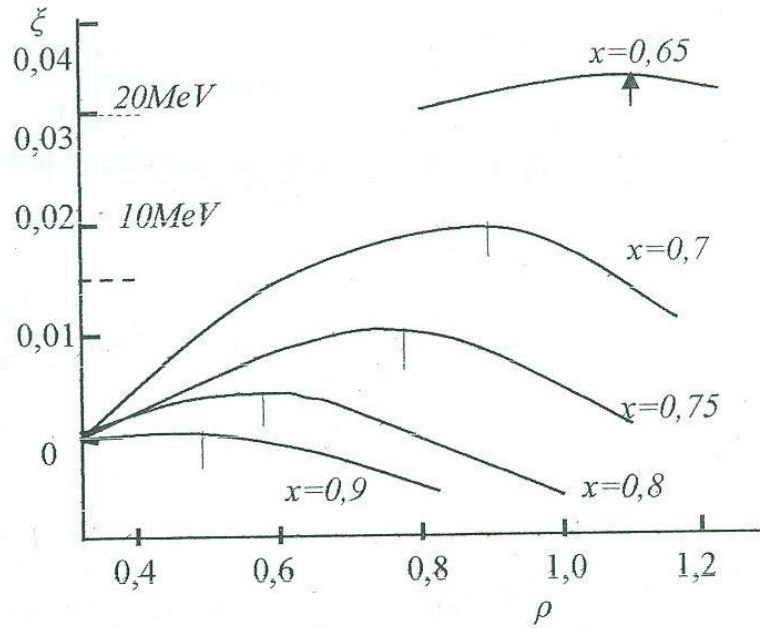
Figure 2.5. Potential energy difference of a uniformly charged liquid drop for different values of facility parameters x. on the left side of the horizontal axis parameter $\xi = \frac{\Delta E}{\Delta E_s^0}$ is indicated versus parameter $\rho = \frac{d}{r_0}$ [21]. On the right side of the horizontal axis deformation energies are indicated. Arrows are indicate saddle points.

2.1.3 The double humped fission barrier

In the beginning of this chapter in 2.1 we have discussed the dependence of nuclear binding energy on nuclear deformation and stated that in a simple liquid drop model (LDM) the nuclear deformation energy (potential energy difference of deformed and spherical nucleus in fission) is due to the surface and Coulomb energy changes in deformation. But this model doesn't take into account the shell structure of the nucleus.

Strutinsky [23] has considered nuclear Shell effects to the deformation energy.

The shell correction effect to the LDM binding energy was taken into account by considering a small division from a uniform distribution of nucleolus in the phase space (coordinate and momentum space) of nucleolus. The energy difference due to the shell effects of a nucleus is expressed as

14

$$\delta U = U - \tilde{U} \tag{2.1.18}$$

where

$$U = \sum_v \varepsilon_v 2n_v \tag{2.1.19}$$

is the sum of energies of nucleons over all occupied single- particle states, ε_v are nucleon levels in the average nuclear potential and the n_v is the occuption numbers. In Eq.(2.1.18)

$$\tilde{U} = 2 \int_{-\infty}^{\lambda} E\, \tilde{g}\,(E)\, dE \tag{2.1.20}$$

is the energy of uniformly distributed nucleons, $\tilde{g}\,(E)$ is uniform distribution of nucleon states and λ is the corresponding chemical potential.

Total binding energies , which takes into account the sell effects can be written as a sum of the LDM binding energy(B_{LDM}), the residual interaction energy in the form of nucleon paring energy interaction (δP) and the shell correction energy δU , as

$$B = B_{LDM} + \sum_{p,n}(\delta U + \delta P) = B_{LDM} + \delta U + \delta P \tag{2.1.21}$$

The sum is over protons and neutrons. The residual interaction term P is less essential in comparison with the shell effects. All terms in above equation are independent on the deformation. The nuclear deformation energy $\Delta E = B\,(deformed) - B\,(spherical)$ depends then on nuclear deformation parametr(β). The results of shell effects to the deformation energy for the fission of $^{242}_{94}Pu$ is illustrated in figure below.

Deformation energy, MeV

deformation parameter, β
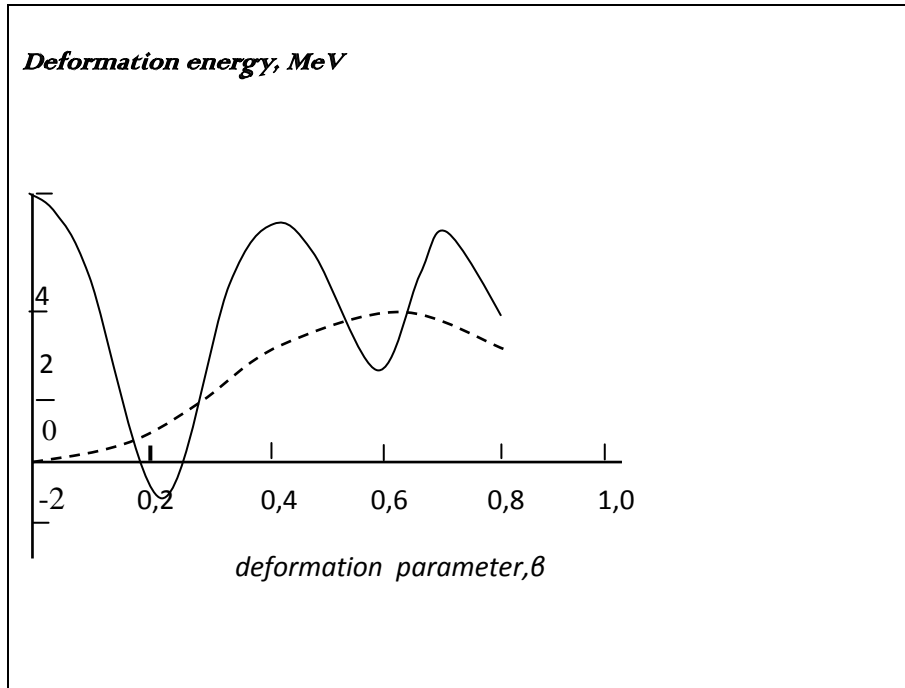
Figure 2.6. Nuclear deformation energy in fission, taking into account the shell effects in Strutinsky model (solid line) and the LDM deformation energy (dashed line) [21].

The first minimum in the deformation energy corresponds to ground state, which turns out to be a few MeV lower than the LDM spherical one. This is an effect of the deformed state shell $N \approx 150,$ which is essential for equilibrium deformations. Due to the second minimum of shell correction the saddle point is strongly deformed and the whole question of the fission barrier is reduced more complicated. In fact, there are two (or even three) fission barriers because a well pronounced minimum appears near the saddle point in the classical fissionable nuclei Th-Cm. This minimum corresponds to deformation $\beta \cong 0.5 - 0.6,$ and may be of importance for the fission process as it provides a possibility for the formation of an intermediate quasi − stationary state in the fissioning nucleus. This minimum is also explains the existence of fissioning isomers.

2.2. Mass distribution of fission fragments in fission of heavy nuclei

Mass distribution from spontaneous and neutron induced fission was investigated in many works (see refs [20]) theoretically and experimentally.

Theory of mass distribution in fission has been given by the authors of work [20]. As sited in this work "The basic assumption of the model used is that the fission fragment distributions can be determined at or near the scission point from the relative potential energies of the complementary nascent fragment pairs ". The total potential energy is given by

$$V = V_1 + V_2 + S_1 + S_1' + S_2 + S_2' + P_1 + P_1' + P_2 + P_2' + V_c + V_n \qquad (2.2.1)$$

The parameter dependences of terms in Eq.(2.1) are given by the relations
$V_1 = V_{LD1} (N_1, Z_1, \beta_1)$, $V_2 = V_{LD2} (N_2, Z_2, \beta_2)$, $S_1 = S_{LD1} (N_1, \tau, \beta_1)$,
$S_1' = S_{LD1} (Z_1, \tau, \beta_1)$, $S_2 = S_{LD2} (N_2, \tau, \beta_2)$, $S_2' = S_{LD2} (Z_2, \tau, \beta_2)$,
$P_1 = P_1 (Z_1, \tau, \beta_1), P_1' = P_1' (N_1, \tau, \beta_1), P_2 = P_2 (N_2, \tau, \beta_2), P_2' = P_2'(Z_2, \tau, \beta_2)$.

Here N and Z are neutron and proton numbers, β is the deformation parameter for the complementary fragments 1 and 2. [β is defined in terms of the semi major (c) and semi minor (a) axes of a prolate spheroid with $c = kr_0 A^{\frac{1}{3}} (1 + \frac{2\beta}{3})$ and $a = kr_0 A^{\frac{1}{3}} (1 - \frac{\beta}{3})$ where k is a volume conservation factor, $r_0 = 1.16\ fm$]. d is distance between coaxial spheroids of fission fragments , the liquid- drop energies (V_{LD}) and the shell (S) and pairing (P) corrections all include their dependence on deformation β. The dependence of the shell and pairing corrections on the intrinsic single-particle excitation τ is also indicated.

The mutual coulomb interaction V_c of two spheroids of charge $Z_1 e$ and $Z_2 e$ is given by

$$V_c = \frac{Z_1 Z_2 e^2 F}{D} \qquad (2.2.2)$$

where F($\approx 1.0 - 1.1$) is a shape factor representing the difference between the coulomb interaction of two uniformly charged spheroids and that of two point charges separated by a distance D.

The nuclear interaction energy is given for two no overlapping spheres of radii R_1 and R_2 with a center of mass distance $D \geq R_1 + R_2$ as supposed by H.J.Krappe and J.R. Nix in Ref [24]

$$V_n = -4 \left(\frac{a}{r_0}\right)^2 a_s(1 - k_s I^2) \left(\frac{R_1}{a} \cosh\frac{R_1}{a} - \sinh\frac{R_1}{a}\right)$$

$$\times \left(\frac{R_2}{a} \cosh\frac{R_2}{a} - \sinh\frac{R_2}{a}\right)\frac{e^{-D/a}}{D/a}, \qquad (2.2.3)$$

where a= 1.4 fm , $a_s = 24.7\ MeV$, $k_s = 4.0$.

The shell corrections have been calculated with the Strutinski model [23] by use of Wood-Saxon potential.

The pairing correction energy was calculated using the BCS formalism [25] with the average pairing gap $\overline{\Delta} = \left(11/\sqrt{A}\right) MeV$ for both neutrons and protons at zero temperature.

The relative probability of formation of any fission fragment pair is given by

$$P(N, Z, \tau, d) = \int_{\beta_1=0}^{\beta_{max}} \int_{\beta_1=0}^{\beta_{max}} \exp[-V(N, Z, \beta, \tau, d)/T_{coll}]\, d\beta_1 d\beta_2 \qquad (2.2.4)$$

where $V(N, Z, \beta, \tau, d)$ is the value of the potential calculated from Eq.(2.2.1), T_{coll} is the collective temperature which characterized the statistical equilibrium among collective states. The Eq.(2.2.4) is the basic equation of the model of work [20] for the calculation of mass distribution , kinetic energy distribution , and other distributions of fission fragments. This model is well reproduced the general trends of the mass distribution in spontaneous fission of [252]Cf and other fission nuclides.

However, there are several quantitative discrepancies between experimental results and calculation results of the authors of work [21]. Namely, the calculated mass distribution for [252]Cf spontaneous fission is too narrow and the positions of the asymmetric peaks are somewhat displaced, peak -to- valley ratios is too small.

The mass distribution of fission fragments can approximately be expressed by the sum of two Gauss distribution with equal weighting factors, i.e.

$$Y(A) = c \cdot \left[\exp\left\{ -\frac{(A - \overline{A_L})^2}{2\sigma_{A_L}^2} \right\} + \exp\left\{ -\frac{(A - \overline{A_H})^2}{2\sigma_{A_H}^2} \right\} \right] \qquad (2.2.5)$$

In this equation $\overline{A_L}$, $\overline{A_H}$ and $\sigma_{A_L}^2$, $\sigma_{A_H}^2$ are the average mass numbers and mass dispersions, respectively for the light and heavy fragments, c is the normalization constant.

2.3. Experimental mass distribution of fission fragments in spontaneous fission of ^{252}Cf

Detailed experimental data for the mass distribution of fission fragments in spontaneous fission of ^{252}Cf are available in works [16, 17]. Below in Figure 2.7 it is illustrated measured mass distribution from work [17] in the fission fragment mass range 89-164. Data are reconstructed from experimental mass yield curve of this work.
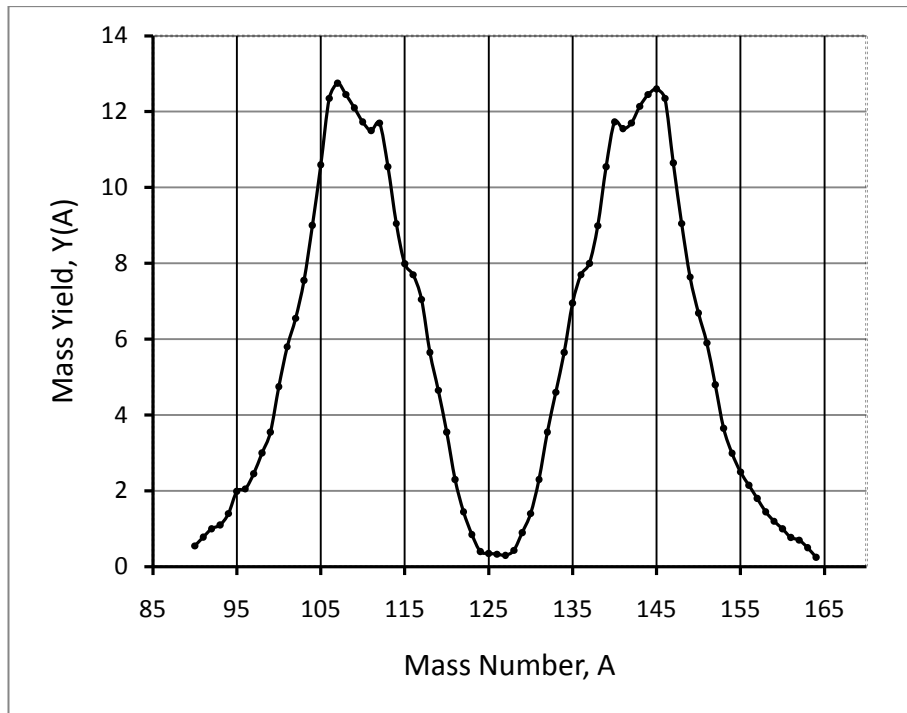
Figure2.7. Mass distribution of fission fragments in spontaneous fission of ^{252}Cf [17] .

Data are given in table below.

Tables 2.1. Mass yield versus mass fission fragment mass as in Fig 2.7

Mass number, A	Mass Yield, Y(A)	Mass number, A	Mass Yield, Y(A)
90	0,5	117	5,54
91	0,6	118	4,43
92	0,7	119	3,7
93	0,93	120	2,78
94	1,13	121	1,84
95	1,41	122	1,19
96	1,65	123	0,71
97	1,89	124	0,33

98	2,27	125	0,31
99	2,78	126	0,31
100	3,7	127	0,25
101	4,56	128	0,31
102	5,14	129	0,64
103	5,93	130	1,09
104	7,03	131	1,77
105	8,35	132	2,77
106	9,74	133	3,62
107	9,94	134	4,42
108	9,8	135	5,46
109	9,52	136	6,03
110	9,22	137	6,26
111	9,07	138	7,05
112	9,22	139	8,27
113	8,34	140	9,2
114	7,11	141	9,05
115	6,27	142	9,2
116	6,06	143	9,5
144	9,74	154	2,33
145	9,89	155	2
146	9,72	156	1,70

147	8,41	157	1,43
148	7,08	158	1,17
149	6,00	159	0,94
150	5,23	160	0,70
151	4,6	161	0,61
152	3,77	162	0,53
153	2,88		

The parameter values in Eq. (2.2.5) for the mass distribution of fission fragments in spontaneous fission of ^{252}Cf measured in the work [27] is estimated from relations

$$\overline{A_L} = \sum_{i=90}^{126} A_L^i \ P_L^i \ , \overline{A_H} = \sum_{i=126}^{162} A_H^i \ P_H^i \qquad (2.3.1\ )$$

$$\sigma_L^2 = \sum_{i=90}^{126} \left(A_L^i - \overline{A_L}\right)^2 \cdot P_L^i \ , \quad \sigma_H^2 = \sum_{i=126}^{162} \left(A_H^i - \overline{A_H}\right)^2 \cdot P_H^i \qquad (\ 2.3.2)$$

for light and heavy fragment groups, respectively. Here P_L^i , P_H^i are the light and heavy mass yields probabilities determined from relations

$$P_L^i = \frac{Y_L^i}{\sum_{i=90}^{126} Y_L^i} \ , \ P_H^i = \frac{Y_H^i}{\sum_{i=126}^{162} Y_H^i} \qquad (\ 2.3.4)$$

Such that $\sum_{i=90}^{126} P_L^i = 1$ and $\sum_{i=126}^{162} P_H^i = 1$.

Results of calculations gives $\overline{A_L} = 107.133$ and $\overline{A_H} = 141.148$ for the average masses and $\sigma_L^2 = 45,06$ and $\sigma_H^2 = 46,11$ for the mass dispersions.

In our investigation of neutron multiplicity and excitation energy correlation between the fission fragments we are choosing three mass ranges of fission fragment masses, according to increasing, approximate constancy and decreasing mass yield behaviors in the mass distribution curve. This ranges are (89-106), (106-112), (112-126) for the light fragment masses and (163-146), (146-140), (140-126) for the complementary heavy fragment masses. We shall use data of the mass yields of fission fragments in spontaneous fission of ^{252}Cf.

2.4. Multi – Model Fission Model

The Multi- Modal Fission Model or the so-called nuclear scission model was given by the authors of work [28]. This model considers the nuclear fission as evolution unstabilities instead of equilibrium fission model given by Bohr and Wheeler. Model concerns exit channels and tens with fragment properties as yield total kinetic energy and so on. The fission channels in this model are suggested to be evaluated by the critical deformation over the fission barrier. Pre-scission shape in the model looks like two beats connected by the neck. Random neck rupture and multi channels calculations supplement each other. Nuclear shape in this model is given by the equation

$$\rho^2(\zeta) = (l^2 - \zeta^2) \sum_n \alpha_n \cdot (\zeta - Z)^n , \qquad (2.4.1)$$

where l, Z are parameters, ζ is cylindrical coordinate.

The experimental data for the mass distribution in spontaneous fission of Cf-252 measured at IRMM [29] has been analyzed in the framework of multi – model fission model [30]. Five fission modes, Standard I (S1), Standard II (S2), Standard III (S3), and Super long (SL), Standart X (SX) with corresponding mass dispersions and waiting percentages are used for description of measured mass distribution. These modes and corresponding parameters values are described in table below.

Table 2.2. The set of multi- modal data used for the calculation of the parameters entering the PFNS model

MODES	$\langle A_H \rangle$	σ_{AH}	W%
S1	135.557	3.184	12.6676
S2	143.031	4.445	46.9569
SX	146.887	7.206	36.2605
S3	157.494	5.346	0.9284

SL	126	14	3.1566
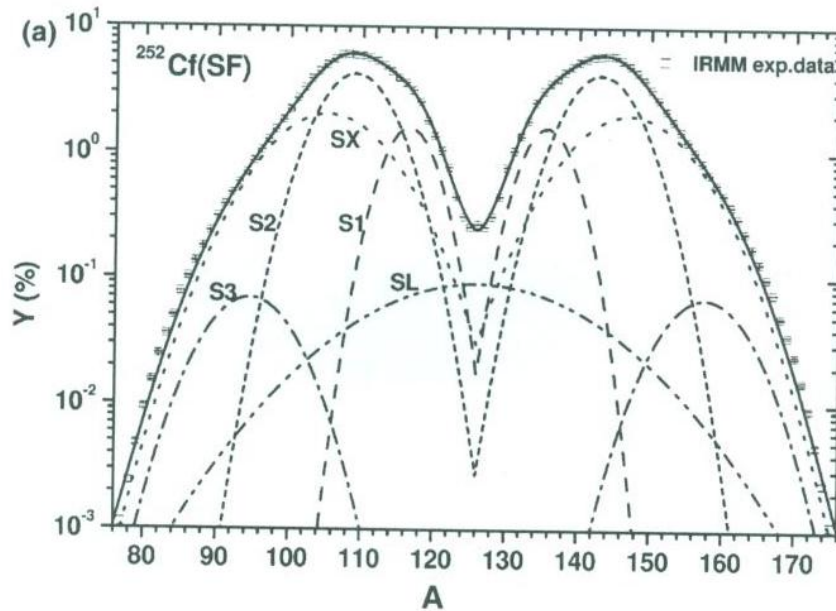
Figure 2.8.The IRMM experimental data [29] of the total fission fragment mass distribution (obtained as a superposition of fission mode mass yields). The fission mode contributions are given in broken line.

In Table 2.2 $\langle A_H \rangle$ is the average mass of heavy fragment, σ_{AH} is the dispersion of mass distribution for heavy fragment of corresponding mode.

Graphical representation of multi – modal mass yields and comparison with experimental mass yield is described in Fig 2.8. Expression for the total and partial mass yields are expressed as

$$Y(A) = \sum_m Y_m(A), \ Y_m(A) = \frac{w_m}{\sigma_{Am} \sqrt{2\pi}} \exp\left(- \frac{(A-\langle A \rangle_m)^2}{2\sigma_{Am}^2}\right), \qquad (2.4.2)$$

Such description of mass distribution in the work of Hambsch et.al. [30] led to the better description of experimental data.

CHAPTER 3

KINETIC ENERGY DISTRIBUTION OF FISSION FRAGMENTS IN SPONTANEOUS FISSION OF ^{252}Cf

In this chapter we shall discuss kinetic energy distribution of fission fragments. This is necessary in order to calculate excitation energy of fission fragments from energy release in given kind of fission.

Here we note that excitation energy of fission fragments can also be found from neutron multiplicity data which will be discussed in Chapter 4. We use experimental data for ^{252}Cf sponteneous fission fragment kinetic energy distribution of work [16]. Then we calculate the energy release in sponteneous fission of ^{252}Cf into the primary light and heavy fission fragments of mass numbers A_L and A_H, respectively in order to find total excitation energy.

3.1. Total energy release in fission (Q-values)

The total energy release in spontenous fission of ^{252}Cf into two complementary fission fragments of mass numbers A_L and A_H, and charge numbers Z_L, and Z_H has form

$$Q = [M(^{252}_{98}Cf) - M(Z_L, A_L) - M(Z_H, A_H)]c^2 \qquad (3.1.1)$$

where

$A_L + A_H = 252$, $Z_L + Z_H = 98$. We note that the masses in the equation (3.1.1) in fact are the masses of excited nuclei and Q-value is a cor

responding energy released in fission. However, these equation can be used for the ground state masses of fission fragments. In this case the above equation (3.1.1) is equivalent to the equation

$$Q = TKE + TEX \,, \tag{3.1.2}$$

where TKE is total kinetic energy and TEX is total excitation energy. In Eq.(3.1.1) Z_L and Z_H values are the most probable values of charges for the fragments of mass A. Below in section 3.1.1 we discuss most probeble charge calculation method.

3.1.1 The most probable charges of fission fragments

The most probable charges for the heavy and light fission fragments in spontaneous fission of Cf-252 may be found according to H.N.Erten, O.Birgül, N,K.Aras Ref [31] as

$$Z^p(L) = Z_0 + 0{,}37 \tag{3.1.3}$$
$$Z^p(H) = Z_0 - 0{,}37 \tag{3.1.4}$$

where $Z_0 = \frac{Z_{fis}}{A_{fis}} \cdot A$ is a charge value in the uniform charge distribution (UCD) model, A is the fission fragments mass, Z_{fis}, A_{fis} are the charge and mass numbers of fissioning nucleus. For the ^{252}Cf spontaneous fission

$$Z_0 = \frac{98}{252} \cdot A = 0{,}3889 \cdot A \tag{3.1.5}$$

İn the table 3.1 it is illustrated the most probable charge values, calculated by the use of equations (3.1.3-3.1.4) in the mass range of fission fragments (73-179) .

Table 3.1. The most probable charges of fission fragments in the mass range (73-179)

Mass number (A)	Charge number in (UCD) model (Z_0)	Most probable charge (Z^p)	Mass number (A)	Charge number in (UCD) model (Z_0)	Most probable charge (Z^p)
73	28,38	29	109	42,38	43
74	28,77	29	110	42,38	43
75	29,16	30	111	43,16	44
76	29,55	30	112	43,55	44
77	29,94	30	113	43,94	44
78	30,33	31	114	44,33	45
79	30,72	31	115	44,72	45
80	31,11	31	116	45,11	45
81	31,49	32	117	45,49	46
82	31,88	32	118	45,88	46
83	32,27	33	119	46,27	47
84	32,66	33	120	46,66	47
85	33,05	33	121	47,65	48
86	33,44	34	122	47,44	48
87	33,83	34	123	47,83	48
88	34,22	35	124	48,22	49
89	34,61	35	125	48,61	49
90	34,99	35	126	48,99	49
91	35,38	36	127	49,38	49
92	35,77	36	128	49,77	49
93	36,16	37	129	50,16	50

94	36,55	37	130	50,55	50
95	36,94	37	131	50,94	51
96	37,33	38	132	51,33	51
97	37,72	38	133	51,72	51
98	38,11	38	134	52,11	52
99	38,49	39	135	52,49	52
100	38,88	39	136	52,88	52
101	39,27	40	137	53,27	53
102	39,66	40	138	53,66	53
103	40,05	40	139	54,05	54
104	40,44	41	140	54,44	54
105	40,83	41	141	54,83	54
106	41,22	42	142	55,22	55
107	41,61	42	143	55,61	55
108	41,99	42	144	55,99	56
145	56,38	56	163	63,38	63
146	56,77	56	164	63,77	63
147	57,16	57	165	64,16	64
148	57,55	57	166	64,55	64
149	57,94	58	167	64,94	65
150	58,33	58	168	65,33	65
151	58,72	58	169	65,72	65
152	59,11	59	170	66,11	66
153	59,49	59	171	66,49	66
154	59,88	60	172	66,88	66
155	60,27	60	173	67,27	67

156	60,66	60	174	67,66	67
157	61,05	61	175	68,05	68
158	61,44	61	176	68,44	68
159	61,83	61	177	68,83	68
160	62,22	62	178	69,22	69
161	62,61	62	179	69,61	69
162	62,99	63			

Next we calculate energy release for different mass division modes in spontaneous fission of ^{252}Cf. For the masses of different fragments we use mass table of G. Audi et al.[32]. The results are shown in the table 3.2.

Table3.2. the Q-values for different mass division modes.

Mass number, A	Q-value (Mev)	Mass number, A	Q-value (Mev)
73	176,622	100	207,133
74	176,156	101	210,99
75	181,303	102	212,601
76	184,675	103	211,102
77	183,408	104	211,39
78	185,245	105	213,728
79	187,646	106	217,29
80	186,566	107	216,393
81	192,453	108	219,11
82	195,322	109	218,244
83	196,011	110	217,511
84	194,614	111	221,022

85	195,201	112	224,506
86	200,974	113	223,882
87	199,085	114	223,994
88	199,868	115	226,75
89	201,228	116	226,276
90	199,3	117	230,393
91	204,32	118	234,064
92	205,237	119	233,53
93	205,501	120	231,355
94	203,682	121	234,408
95	204,262	122	236,907
96	209,502	123	233,942
97	207,298	124	231,269
98	208,37	125	233,504
99	207,864	126	231,669

These table data of Q-values are illustrated in Figures (3.1-3.4) in the seperate mass ranges (73-106), (106-112), (112-126) and total mass range (73-126), respectively for the light fragments masses.
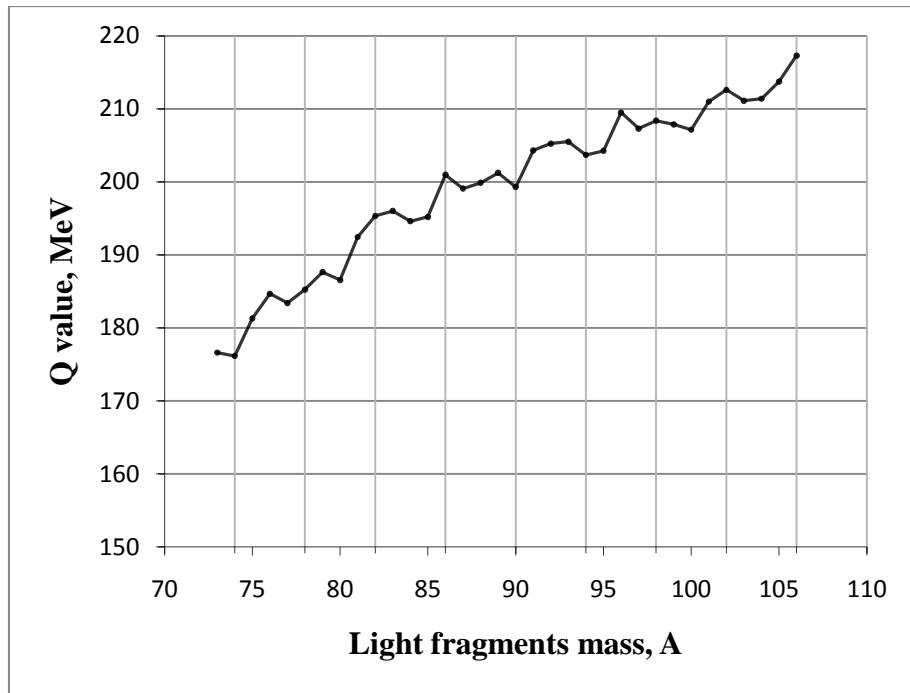
Figure 3.1. The Q-values in the mass range (73-106).
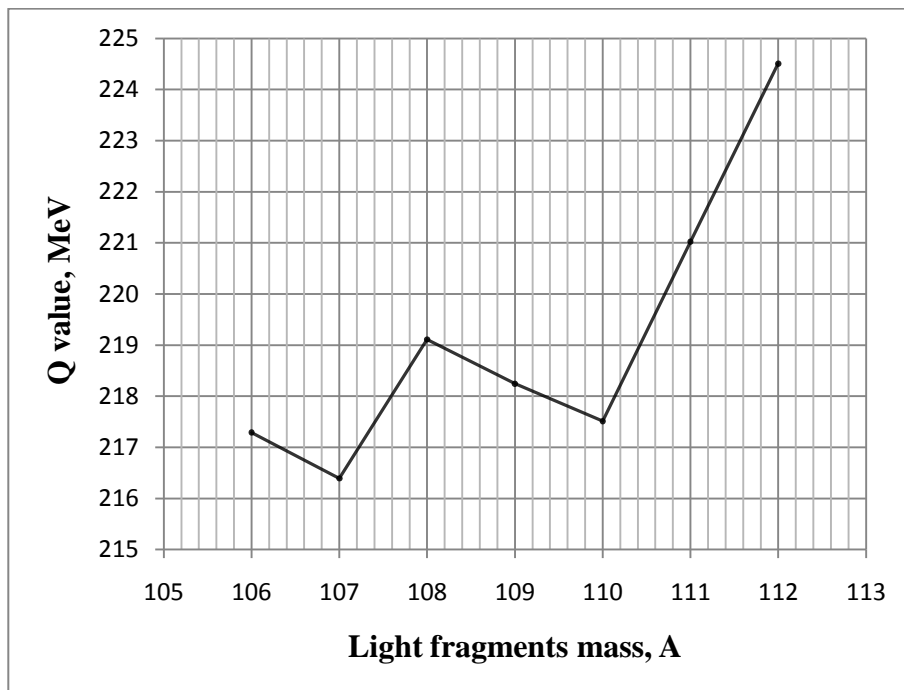
Figure 3.2. The Q-values in the mass range (106-112).
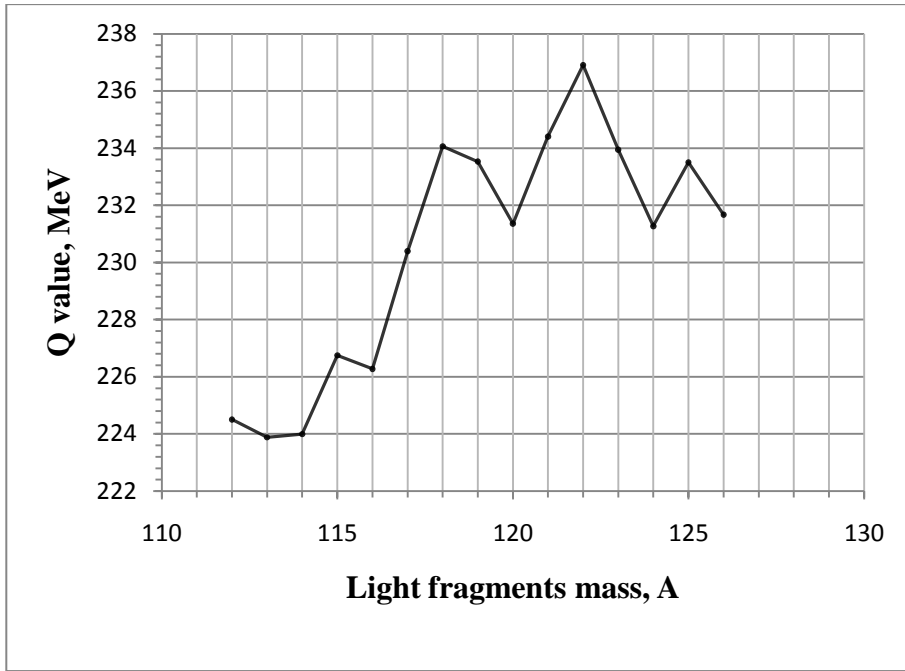
Figure 3.3. The Q-values in the mass range (112-126).
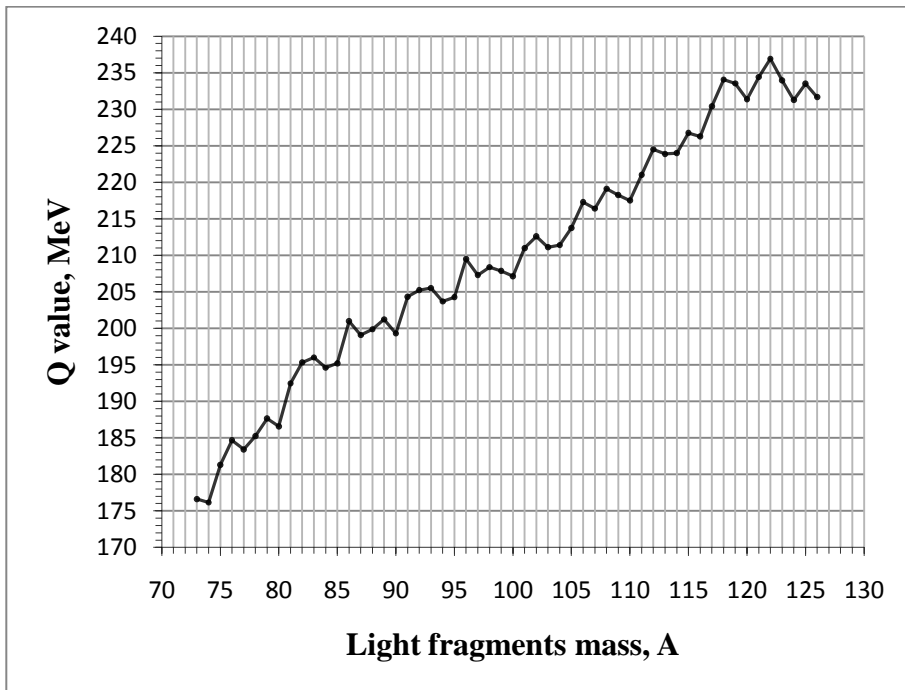
Figure 3.4. The Q-values in the mass range (73-126).

3.2. Total kinetic energy of primary fission fragments

Total kinetic energy of complementary fission fragments in spontaneous fission of ^{252}Cf dependent on fragment mass has been measured in detailed experiment of

33

Kinetter and Budtz- Jorgensen [16]. The results of experimental data of these authors are indicated below in the figures (3.5-3.8), in the total mass range (73-179) , and in the seperate mass ranges (73-106), (106-112), (112-126), respectively for the light fragments masses.

Figure 3.5. Total kinetic energy of fission fragments versus the fragment mass for the spontaneous fission of ^{252}Cf [16].

Figure 3.6. Total kinetic energy of fission fragments versus the fragment mass for the spontaneous fission of ^{252}Cf [16] in the mass range (73-106).
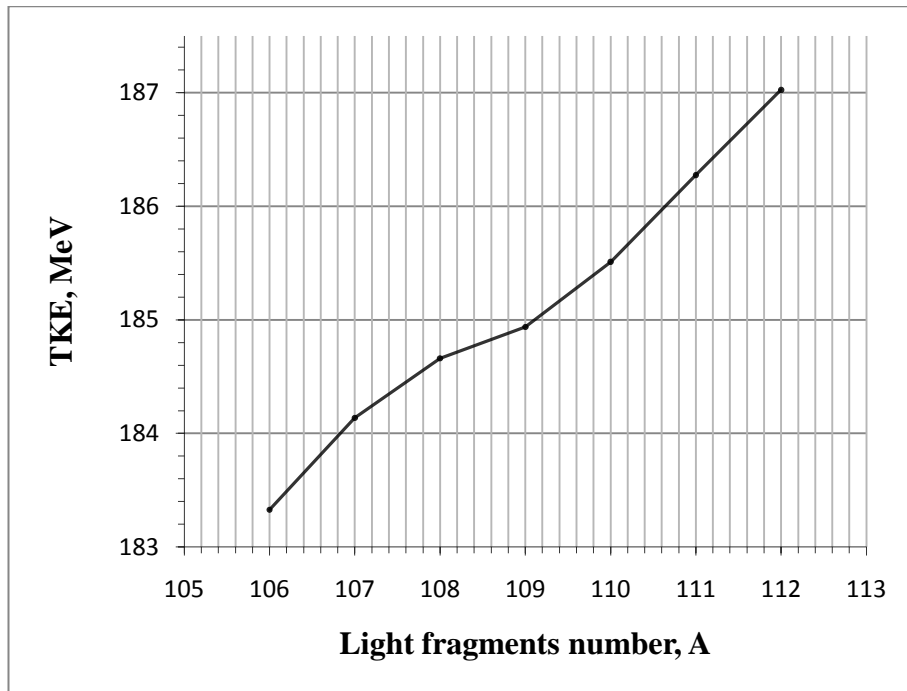
Figure 3.7. Total kinetic energy of fission fragments versus the fragment mass for the spontaneous fission of ^{252}Cf [16] in the mass range (106-112)
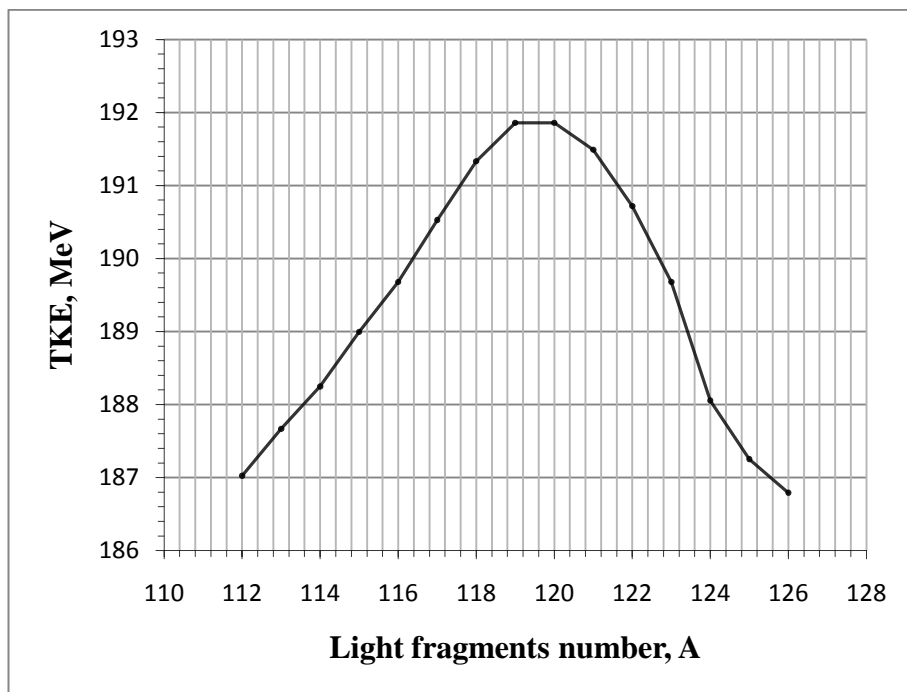
Figure 3.8. Total kinetic energy of fission fragments versus the fragment mass for the spontaneous fission of ^{252}Cf [16] in the mass range (112-126).

The numerical data of total kinetic energies are illustrated in table 3.3.

Table 3.3. Total kinetic energies of fission fragments in spontaneous fission of ^{252}Cf

Mass number, A	TKE (Mev)	Mass number, A	TKE (Mev)
74	150.36076	115	188.99590
75	142.41391	116	189.67969
76	150.54435	117	190.52742
77	151.77490	118	191.33230
78	152.70154	119	191.85755
79	155.59819	120	191.85755
80	158.05710	121	191.49045
81	158.57562	122	190.71856
82	159.33460	123	189.67948
83	159.95856	124	188.05427
84	161.14485	125	187.25187
85	162.36427	126	186.79233
86	163.20410	127	187.34216
87	164.05578	128	188.15899
88	164.90669	129	189.80684
89	165.36175	130	190.77370
90	166.40785	131	191.48582
91	167.38187	132	191.77387
92	168.46716	133	191.73116
93	169.37709	134	191.20187
94	170.26816	135	190.38290
95	171.42469	136	189.51176

96	172.65545	137	188.78099
97	173.77426	138	188.03823
98	174.73168	139	187.44538
99	175.76779	140	186.69799
100	176.90167	141	185.92777
101	178.07718	142	185.14701
102	179.15558	143	184.61031
103	180.11493	144	184.26896
104	181.09590	145	183.67002
105	182.22457	146	182.76219
106	183.32815	147	181.64682
107	184.13636	148	180.49233
108	184.66104	149	179.49155
109	184.93655	150	178.41310
110	185.51034	151	177.29963
111	186.27502	152	176.11994
112	187.02421	153	174.99967
113	187.66766	154	173.96349
114	188.24830	155	172.96478
156	171.85469	168	160.05603
157	170.59410	169	158.92405
158	169.51262	170	158.42289
159	168.62381	171	157.82855
160	167.69984	172	156.68809
161	166.64486	173	155.47872
162	165.49788	174	153.36461

163	164.35679	175	151.75438
164	163.81250	176	149.20491
165	162.82925	177	148.04752
166	162.05719	178	150.82680
167	161.22350		

3.3. The average total kinetic energy of primary fission fragments

For the given type of ^{252}Cf spontaneous fission into the complementary masses we must average total kinetic energy. The total average kinetic energy, then is

$$\overline{TKE}(A_L, A_H) = 0.5\,[TKE\,(A_L) + \,TKE(A_H)] \qquad (3.3.1)$$

Figures below 3.9- 3.12 illustrate total average kinetic energy of fission fragments calculated by use of Eq.(3.7)
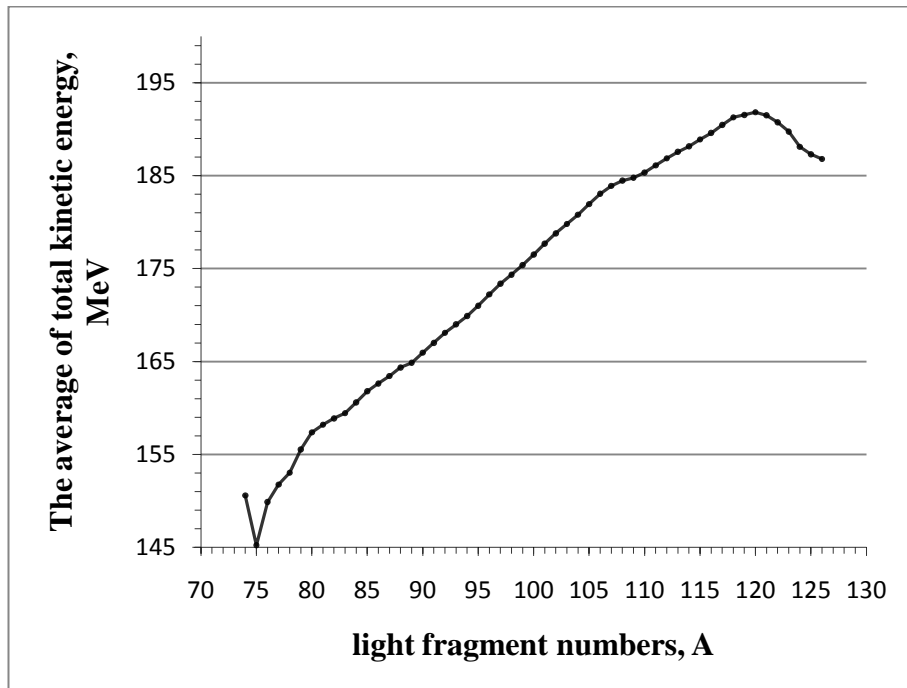
Figure 3.9. The total average kinetic energy of fission fragments versus the fragment mass for the spontaneous fission of Cf-252 [16].
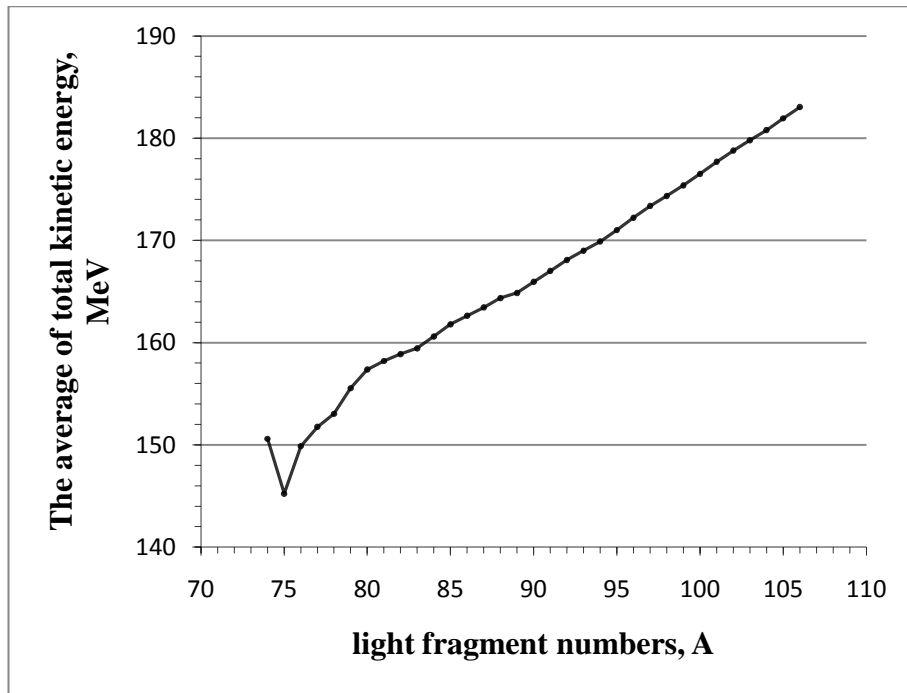
Figure 3.10. The total average kinetic energy of fission fragments versus the fragment mass for the spontaneous fission of ^{252}Cf [16]in the mass range (73-106).
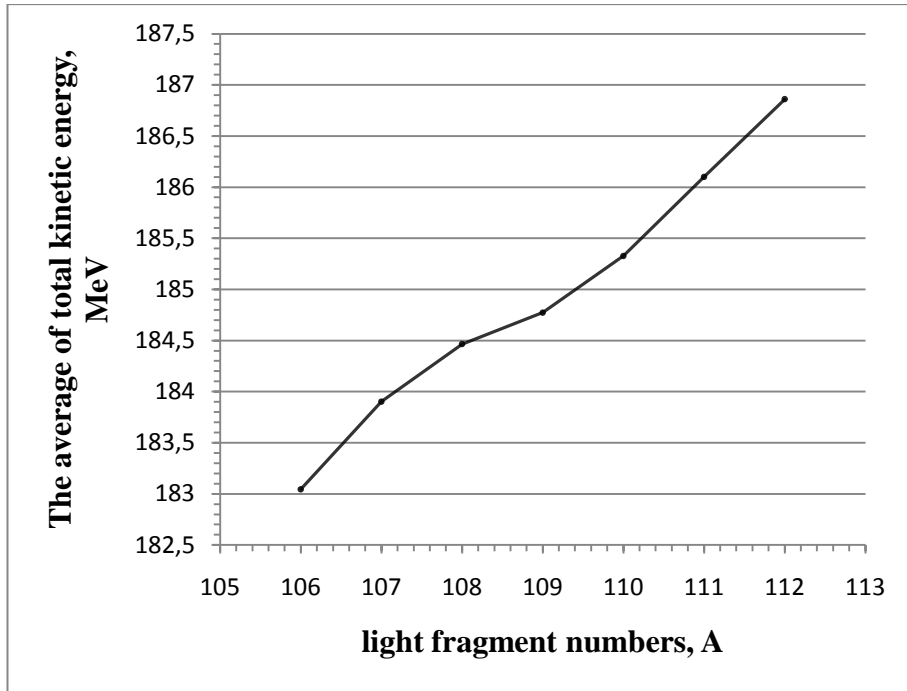
Figure 3.11. The total average kinetic energy of fission fragments versus the fragment mass for the spontaneous fission of ^{252}Cf [16] in the mass range (106-112)
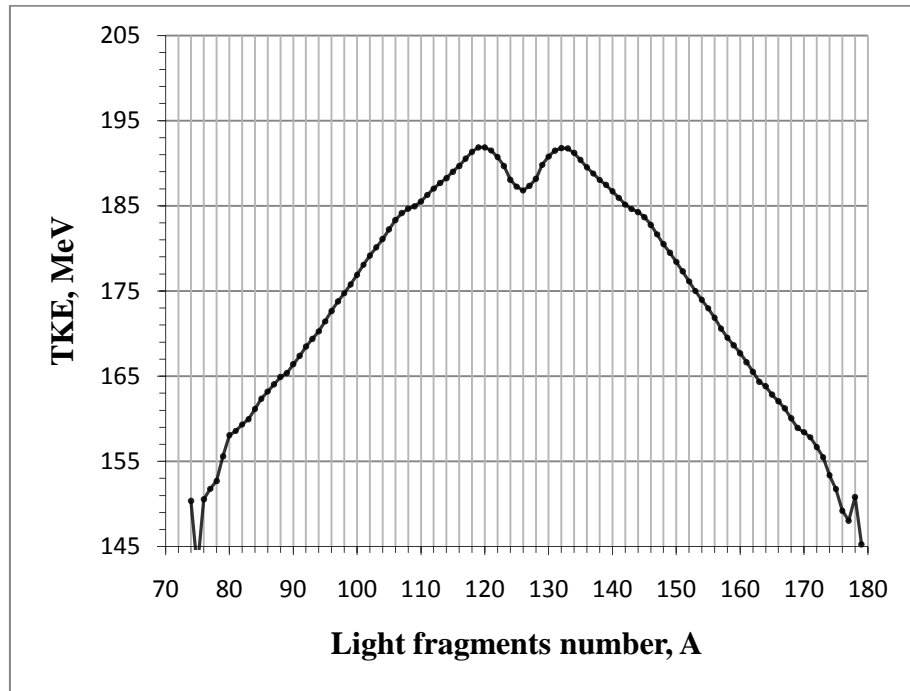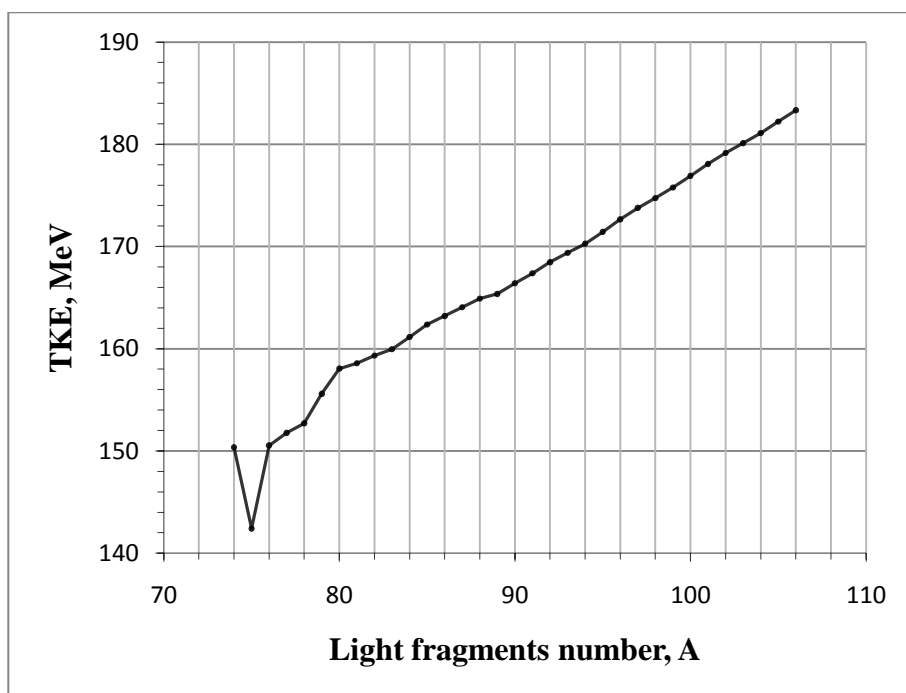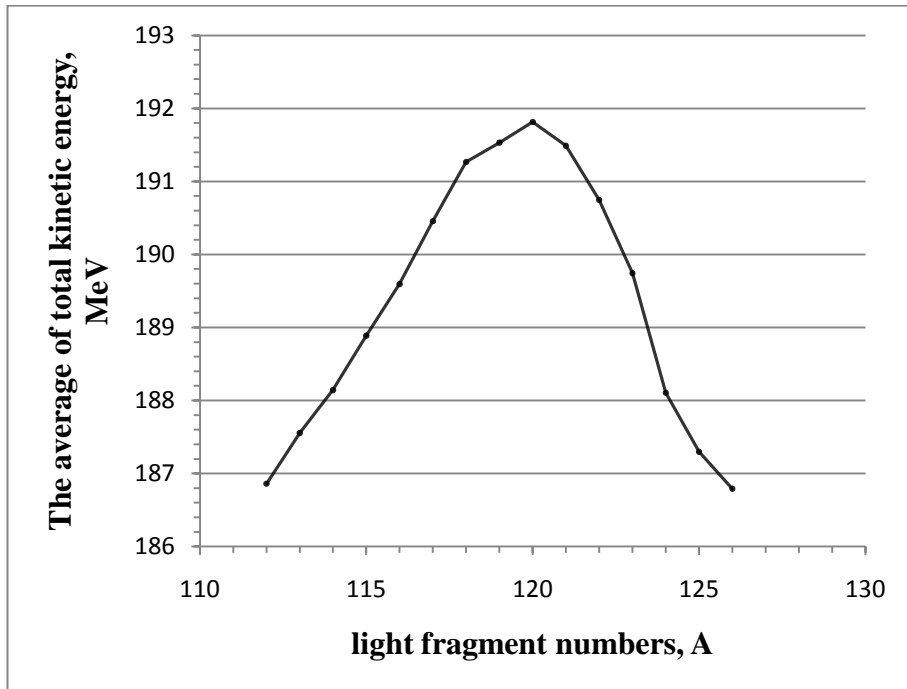

Figure3.12. The total average kinetic energy of fission fragments versus the fragment mass for the spontaneous fission of ^{252}Cf [16] in the mass range (112-126).

The numerical data of the average total kinetic energies are illustrated in table 3.4.

Table 3.4. Total avaerage kinetic energies of fission fragments in spontaneous fission of ^{252}Cf

Mass number, A	$\overline{TKE}$, MeV	Mass number, A	$\overline{TKE}$, MeV
73	0,0000	102	178,784
74	150,593	103	179,803
75	145,230	104	180,794
76	139,874	105	181,935
77	151,764	106	183.045
78	153,033	107	183,903
79	155,538	108	184,465
80	152,315	109	184,773
81	158,202	110	185,328
82	158,878	111	186,101
83	159,441	112	187,024
84	160,600	113	187,556
85	161,793	114	188,248
86	162,630	115	188,995
87	163,442	116	189,679
88	164,359	117	190,455
89	164,859	118	191,267
90	165,952	119	191,531
91	167,013	120	191,815
92	168,083	121	191,488
93	169,000	122	190,716

94	169,890	123	189,743
95	171,009	124	188,106
96	172,255	125	187,297
97	173,369	126	186,792
98	174,347		
99	175,383		
100	176,510		
101	177,688		

Total excitation energy of fission fragments calculated from expression 3.1.2 are shown in table 3.5.

Table 3.5. Total excitation energy fission fragments in spontaneous fission of ^{252}Cf

Mass number, A	TXE, (Mev)	Mass number, A	TXE, (Mev)
73	0,000	100	30,623
74	25,563	101	33,302
75	36,073	102	33,817
76	34,801	103	31,299
77	31,644	104	30,596
78	32,212	105	31,793
79	32,108	106	33,387
80	28,364	107	32,490
81	33.575	108	34,645

82	36,444	109	33,471
83	36,570	110	32,183
84	34,014	111	34,921
85	33,408	112	37,482
86	38,344	113	36,326
87	35,643	114	35,746
88	35,509	115	37,755
89	36,369	116	36,597
90	33,348	117	39,938
91	37,307	118	42,797
92	37,154	119	41,999
93	36,501	120	39,540
94	33,792	121	42,920
95	33,253	122	46,161
96	37,247	123	44,199
97	33,929	124	43,163
98	34,023	125	46,207
99	32,481	126	44,877

3.4.Total kinetic energy distribution of fission fragments

The total kinetic energy distribution of fission fragments in the fission of different heavy nuclei have been investigated in many works (see, Refs [33-34]). According to these experimental data total kinetic energy distribution may be expressed by nourmal distribution (Gaussian) as

$$P(TKE) = c \cdot \exp\left(-\frac{(TKE-\overline{TKE})^2}{2\sigma_{TKE}^2}\right) \tag{3.4.1}$$

where c is the normalization constant , $\overline{TKE}$ and σ_{TKE} are average total kinetic energy and mean square division of total kinetic energy, respectively. If we suppose independent distribution of total kinetic energy between the complementary fission fragments then kinetic energy distribution of light and heavy fragments may be approximated as

$$P_L(E) = c_L . \exp\left(-\frac{(E_L - \overline{E_L})^2}{2\sigma_L^2}\right) \tag{3.4.2}$$

$$P_H(E) = c_H . \exp\left(-\frac{(E_H - \overline{E_H})^2}{2\sigma_H^2}\right) \tag{3.4.3}$$

where $\overline{E_L} + \overline{E_H} = \overline{TKE}$, $E_L + E_H = TKE$ and $\sigma_L^2 + \sigma_H^2 = \sigma_{TKE}^2$.

Indeed, for independent distribution of kinetic energies between the fission fragments one can write the total kinetic energy distribution

$$P(TKE) = \int_0^\infty P_L(E_L) . P_L(E_H) dE_L = \int_0^\infty P_L(E_L) . P_L(TKE - E_L) dE_L \tag{3.4.4}$$

Substitution of Eqs. (3.4.2 -3.4.3) into the integral of Eq.(3.4.4) gives Eq.(3.4.1).

Normalization constants c, c_L and c_H are defined from conditions

$$\int_0^\infty P(TKE) d(TKE) = 1 \tag{3.4.5}$$

$$\int_0^\infty P_L(E_L) d(E_L) = 1 \tag{3.4.6}$$

$$\int_0^\infty P_H(E_H) d(E_H) = 1 \tag{3.4.7}$$

Solving integrals and using the condition $\overline{E}/\sqrt{2}\,\sigma \sim 10$, we find

$$c = \frac{1}{\sqrt{2\pi}\,\sigma_{TKE}} , c_L = \frac{1}{\sqrt{2\pi}\,\sigma_L} , c_H = \frac{1}{\sqrt{2\pi}\,\sigma_H} \tag{3.4.8}$$

3.5. Neutron multiplicity dependence on total kinetic energy of fission fragments and neutron number correlation

Correlation between numbers of neutron emitted from complementary fission fragments is key property for understanding of partition of excitation energy between the fragments. It was assumed [21] that neutron yields are uncorrelated if total kinetic energy of complementary fission fragments is not fixed. In the experimental work [38] average value of neutron yields product $\overline{\nu_L \cdot \nu_H}$ from complementary fragments in thermal neutron fission of ^{235}U has been measured and result is to be found 1,53. The calculated value of this product given by the expression

$$\overline{\nu_L \cdot \nu_H} = \sum_i \nu_L^i \; \nu_H^i \; p_L^i \; p_H^i, \tag{3.5.1}$$

and based on assumption of independent yield (no correlation), where $P_{H,L}^i$ are corresponding yield weights, gives 1,82. Discrepancy in the calculated and measured values has been composed the reason for the presence of anticorrelation.

Direct measurement of neutron number dispersions in spontaneous fission of ^{252}Cf [39], as indicated in work [21], gave $\sigma_L^2 = 1,108$, $\sigma_H^2 = 1,446$, and $\sigma_T^2 = 1,55$ for the light and heavy fragments and for the total number of neutrons from both fragments, respectively. Using data above, correlation coefficient $\rho_{L,H}$ finding from relation

$$\sigma_T^2 = \sigma_H^2 + \sigma_L^2 + 2\rho_{L,H}\sigma_L\sigma_H \tag{3.5.2}$$

gives $\rho_{L,H} \cong -0,4$, which means relatively slow anticorrelation between the neutron numbers.

In the work [26] mean value of neutron number as a function of mass and total kinetic energy of fission fragments, neutron number variances is measured and detailed analyses of similar measured data of works [40,41] in spontaneous fission of ^{252}Cf has been made. In Figure 3.13, and Figure 3.14 it is illustrated total kinetic energy dependent average neutron multiplicitiesν_L, ν_H and total kinetic energy distribution, respectively for the mass split $A_L = 108$, $A_H = 144$ reproduced from graph of figure 3 of work [26]. In the same figure of work [26] neutron number

45

dispersions and covariances between neutron numbers dependent on total kinetic energy are also illustrated.
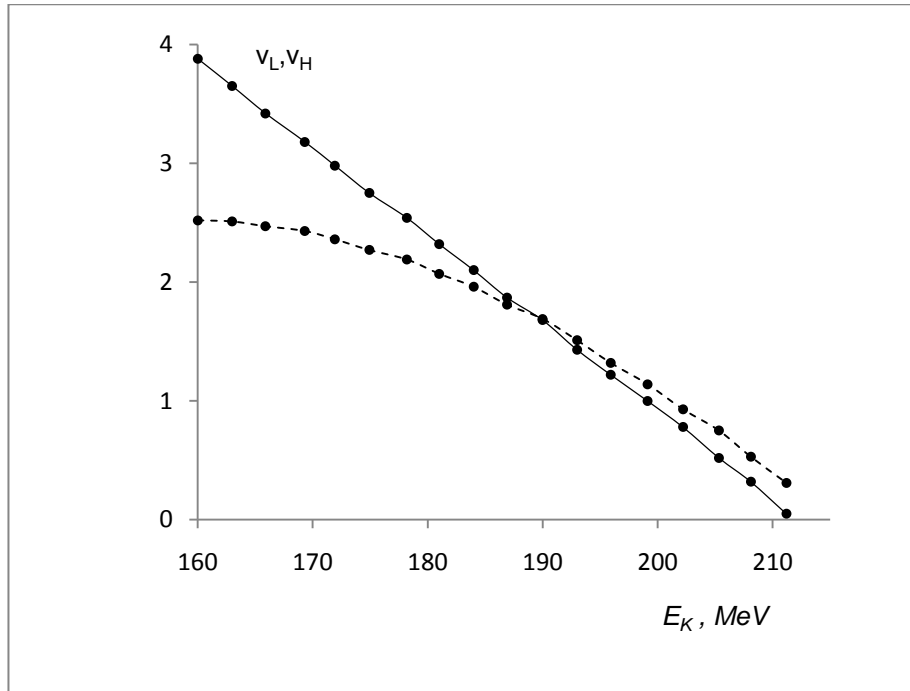
Figure3.13. Experimental data [4] for neutron mean values ν_L (solid curve),   and ν_H (dashed curve) dependent on total kinetic energy of fission fragments for the mass split $A_L = 108$, $A_H = 144$ in spontaneous fission of ^{252}Cf

We analyze these data to find neutron average number correlation ρ_{ν_L,ν_H} for the mass split $A_L = 108$, $A_H = 144$ by using the expression

$$\rho_{\nu_L,\nu_H} = \frac{Cov\ (\nu_L,\nu_H)}{\sigma_{\nu_L} \cdot \sigma_{\nu_H}} \tag{3.5.3}$$

$$Cov\ (\nu_L, \nu_H) = \sum(\nu_L^i - \overline{\nu_L})\ (\nu_H^i - \overline{\nu_H})\ p\ (\nu_L^i)\ p\ (\nu_H^i) \tag{3.5.4}$$

$$\sigma^2(\nu_L) = \sum(\nu_L^i - \overline{\nu_L})^2\ p\ (\nu_L^i) \tag{3.5.5}$$

$$\overline{\nu_L} = \sum \nu_L^i\ p\ (\nu_L^i) \tag{3.5.6}$$
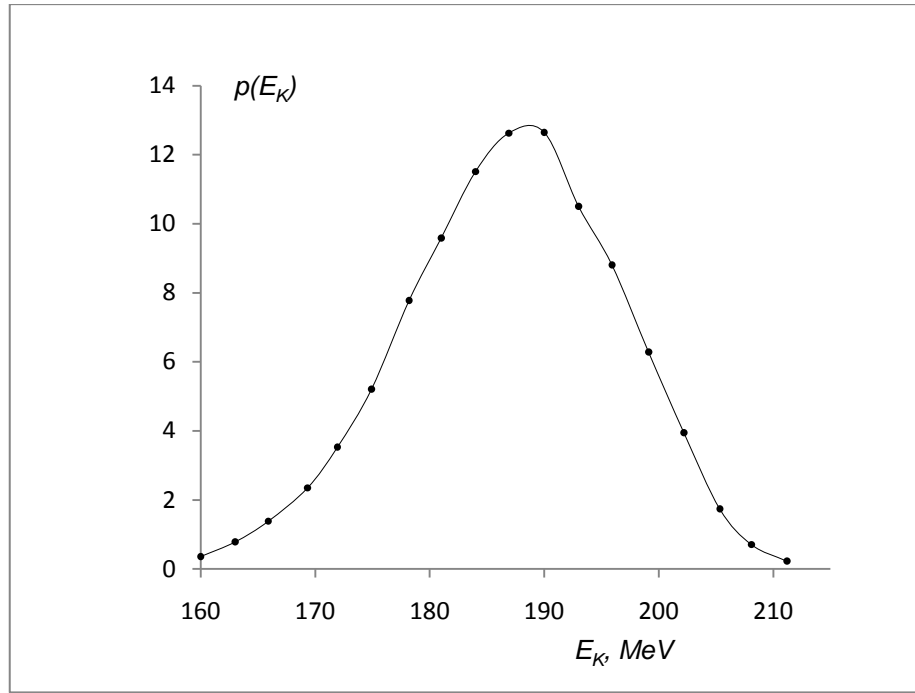
Figure3.14. Total kinetic energy distribution of fission fragments in the mass split $A_L = 108$, $A_H = 144$ in spontaneous fission of ^{252}Cf

Average neutron yields in the above formulas are equal to the kinetic energy yields, namely $p\left(v_L^i\right) = p\left(v_H^i\right) = p\left(E_K^i\right)$. Estimation of neutron average numbers using experimental data of work [26] gives values $\overline{v_L} = 1{,}89$ and $\overline{v_H} = 1.76$ for the mass $A_L = 108$ and $A_H = 144$, respectively. These data are close to those of work [16]. Neutron number dispersions and correlation coefficients are $\sigma_{\overline{v_L}} = 0{,}685$ and $\sigma_{\overline{v_H}} = 0{,}697$, $\rho_{\overline{v_L},v_H} = 0{,}0296$.

CHAPTER 4

NEUTRON AVERAGE MULTIPLICITY AND CORRELATION COEFFICIENT FOR DISTRIBUTION OF $\bar{\nu}(A)$ IN DIFFERENT MASS RANGES OF COMPLEMENTARY FISSION FRAGMENTS

Neutron multiplicity (or neutron average number) has great importance in nuclear reactor calculations. Besides, the neutron multiplicity dependence on fission fragment mass number is an important knowledge for the understanding of fission mechanism and neutron emission from fission fragments. This quantity gives also basic information about the sharing of excitation energy between the fission fragments, which we will discuss in the next chapter.

Main contribution to the fission fragment of excitation energy is due to emitted from fragment neutron energy and this energy is related with neutron average multiplicity. Therefore we shall discuss neutron average multiplicity dependent on fragment mass and its correlation for the complementary fission fragments.

In Figure (4.1), it is illustrated the neutron multiplicity dependence on fission fragment mass in spontaneous fission of $^{252}_{92}Cf$, observed in the experiments of work [16]. As seen in the graph neutron multiplicity has triple "sawtooth" character. This behavior of neutron multiplicity is related with excitation energy of fission fragments. We shall investigate these data in order to get correlation coefficient for neutron number distribution between the complementary fission fragments and then shall found correlation coefficient for the excitation energy distribution between the fission fragments by using equations below.
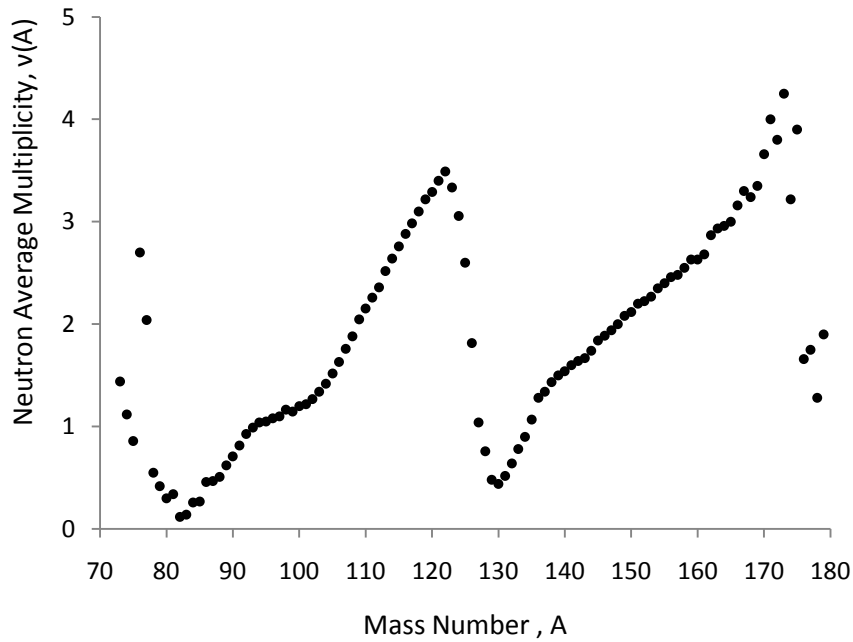
Figure 4.1. Neutron average multiplicity versus fission fragment mass number in spontaneous fission of ^{252}Cf (experimental data of C.Budtz-Jorgensen and K.Knitter, 1988).

In general, the excitation energy consists of internal excitation energy and deformation energy at scission and it is mostly dissipated by neutron and γ emission. However, the internal excitation energy at scission in generally small compared with the deformation energy in the low energy fission, and the energy dissipated by γ ray emission is less than the neutron binding energy, that is independent of total kinetic energy and is related with $\bar{\nu}(A)$ in thermal neutron-induced fission and spontaneous fission of actinides.

In figure 2.7 of chapter 2, we illustrate mass distribution of fission fragments in spontaneous fission of ^{252}Cf taken from work [26]. In order to calculate correlation coefficient mentioned above we divide mass region of fission fragments into three parts where mass yields have monotonic character. These regions are:

1. The light fragment mass range (73-106), and complementary heavy fragment mass range (146-179), where mass yields monotonically is increasing for light mass region and decreasing for heavy mass region,

2. The light fragment mass range (106-112), and complementary heavy fragment mass region (140-146), where mass yields approximately are constant for each region,

3. The light fragment mass range (112-126), and complementary heavy fragment mass range (126-140), where mass yields monotonically is decreasing for light mass range and increasing for heavy mass range.

In addition, we shall consider whole light fragment mass range (73-126), and complementary whole heavy fragment mass range (126-179)

4.1. Correlation coefficients for distribution of $\bar{v}(A)$ in different mass ranges of complementary fission fragments

Let us have two sets of variables $x_i \in X$ and $y_i \in Y$. We take equal number of variables in these sets. The correlation between these variables may be determined by the so-called Pirson correlation coefficient as:

$$r_{xy} = \frac{\sum_{i=1}^{n}(x_i - \bar{x}_i)(y_i - \bar{y}_i)}{\sqrt{\sum_{i=1}^{n}(x_i - \bar{x}_i)^2 \sum_{i=1}^{n}(y_i - \bar{y}_i)^2}} \qquad (4.1.1)$$

where $\bar{x}_i = \frac{1}{n}\sum_{i=1}^{n} x_i$ and $\bar{y}_i = \frac{1}{n}\sum_{i=1}^{n} y_i$. We apply this relation to find correlation coefficient between $\bar{v}(A)$ taken from light and complementary heavy mass ranges, mentioned above in items 1, 2 and 3, respectively. In other worlds we take $\bar{v}(A_i^L) \rightarrow x_i \in (73 - 106)$, $\bar{v}(A_i^H) \rightarrow y_i \in (146 - 179)$ for the item number one, where letters L and H refer light and heavy fragments. Correlation coefficient calculated using Eq(4.1.1) in this case gives

$$r_{xy} = -0.633373. \qquad (4.1.2)$$

Below in the Figure 4.2 it is illustrated correlation of neutron multiplicities from complementary fission fragments in the light fragment mass range $(73 - 106)$, and heavy fragment mass range $(146 - 179)$. The correlation coefficient value may be understood when thought multiplicity behaviors below A=81.

Figure 4.2. Neutron multiplicities from complementary fission fragments in the light fragment mass range$(73 - 106)$ (dashed curve), and heavy fragment mass range $(146 - 179)$ (solid curve)

This value means that, the relation between light and complementary heavy fragments is strong but negative because the first one is increase and the other is decrease.

Now let us to apply this relation to find correlation coefficient between $\bar{v}(A)$ taken from light and complementary heavy mass ranges in the region 2 we take $\bar{v}(A_i) \rightarrow x_i(106 - 112), \bar{v}(A_i) \rightarrow y_i \in (140 - 146)$, Correlation coefficient calculated by using Eq.(4.1.1) in this case gives

$$r_{xy} = -0.993743 \tag{4.1.3}$$

This value means that, the relation between light and complementary heavy fragments has a prefect strong negative because where mass yields approximately are constant (symmetric values) for each region, this value is approximately near to (-1) and this is the greater number of correlation but negative.

51

Below in the Figure 4.3 it is illustrated correlation of neutron multiplicities from complementary fission fragments in the light fragment mass range$(106 - 112)$, and heavy fragment mass range $(140 - 146)$. The correlation coefficient value may be understood when thought multiplicity behaviors below A=106.
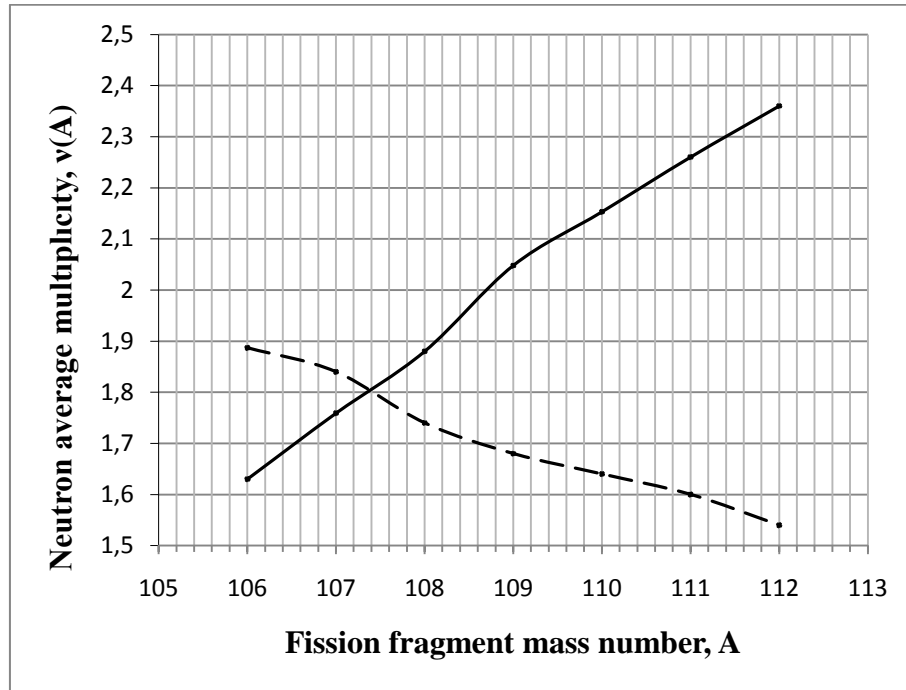
Figure 4.3. Neutron multiplicities from complementary fission fragments in the light fragment mass range$(106 - 112)$ (dashed curve), and heavy fragment mass range $(140 - 146)$ (solid curve)

For the end part when we apply this relation to find correlation coefficient between $\bar{v}(A)$ taken from light and complementary heavy mass ranges, in other worlds we take $\bar{v}(A_i) \rightarrow x_i (112 - 126), \bar{v}(A_i) \rightarrow y_i \in (126 - 140)$, Correlation coefficient calculated by using Eq.(4.1.1) in this case gives

$$r_{xy} = -0.940186 \qquad (4.1.4)$$

This value means that, the relation between the neutron average multiplicities of fragment pair is strong but negative. This is illustrated if Fig 4.3.

Below in the Figure 4.4 it is illustrated correlation of neutron multiplicities from complementary fission fragments in the light fragment mass range$(112 - 126)$, and

heavy fragment mass range$(126 - 140)$. The correlation coefficient value may be understood when thought multiplicity behaviors below A=112.
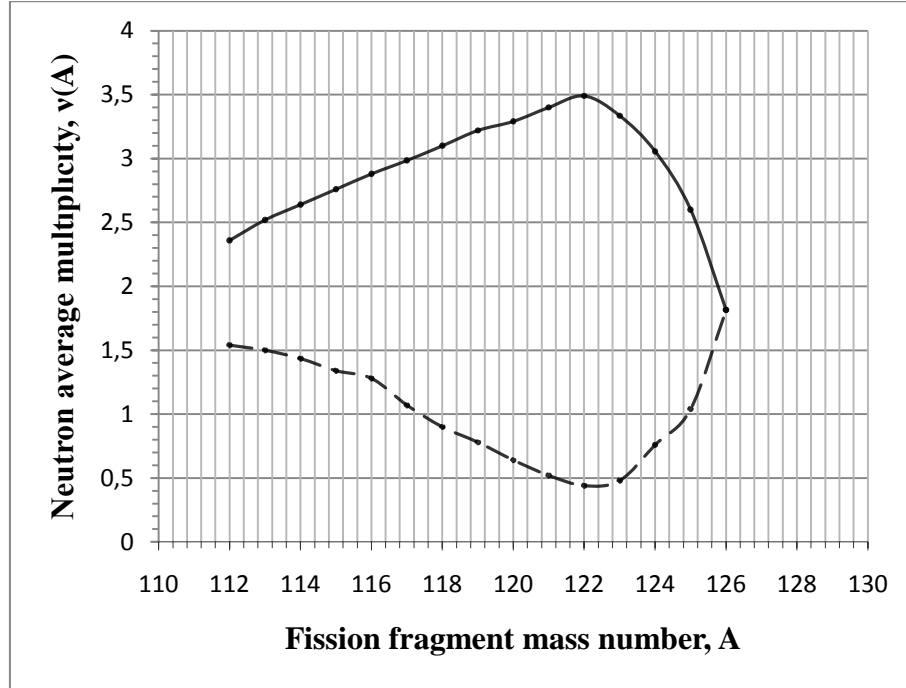
Figure 4.4. Neutron multiplicities from complementary fission fragments in the light fragment mass range$(112 - 126)$ (dashed curve), and heavy fragment mass range $(126 - 140)$ (solid curve)

Let us apply relation 4.1.1 to find correlation coefficient between $\bar{v}(A)$ taken from all values of light and complementary heavy mass ranges, in other worlds we take $\bar{v}(A_i^L) \rightarrow x_i \in (73 - 126)$, $\bar{v}(A_i^H) \rightarrow y_i \in (126 - 179)$ for the item number one , Correlation coefficient calculated using Eq.(4.1.1) in this case gives

$$r_{xy} = -0.883037 \qquad (4.1.5)$$

Below in the Figure 4.5 it is illustrated correlation of neutron multiplicities from complementary fission fragments in the light fragment mass range$(73 - 126)$, and heavy fragment mass range $(126 - 179)$. The correlation coefficient value may be understood when thought multiplicity behaviors below A=81 to A=106, A=106 to A=112, A=112 to A=122 .
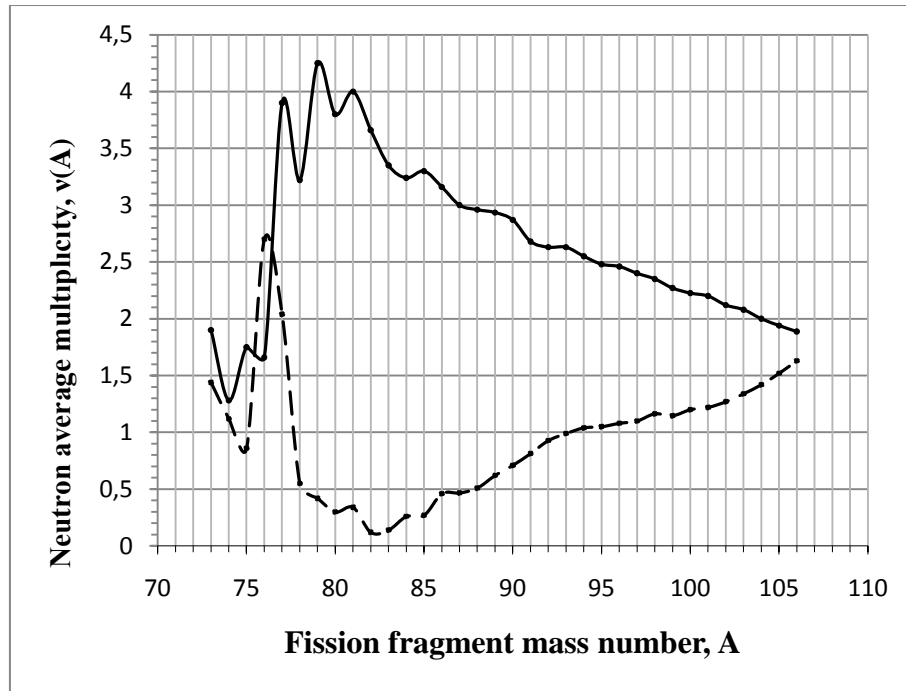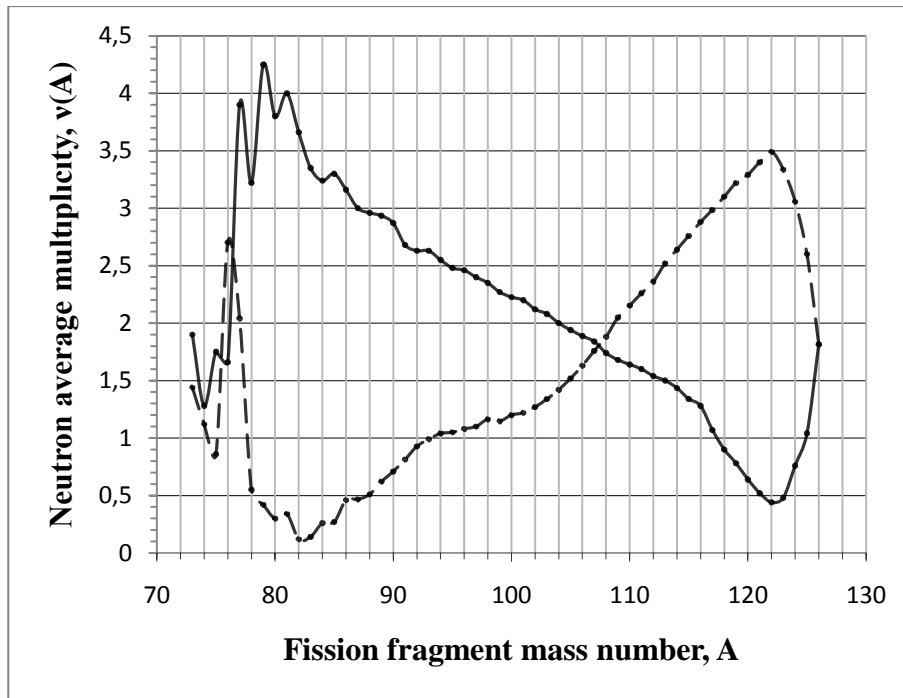
Figure 4.5. Neutron multiplicities from complementary fission fragments in the light fragment mass range$(73 - 126)$ (dashed curve), and heavy fragment mass range $(126 - 179)$ (solid curve)

Below in table 4.1 it is illustrated correlation coefficient values for different mass ranges. From table it is seen that correlation coefficient is close to -1 (r_{xy}= -0.993743) for the mass range $A_l \in (106 - 112)$, $A_h \in (140 - 146)$, in other worlds we find complete approximate anti correlation . Similar anti correlation is valid for the mass range $A_l \in (112 - 126)$, $A_h \in (126 - 140)$. These results are due to strong anti correlation in the partitition of the excitation energy between the fission fragments.

Table 4.1.Pearson correlation coefficient of neutron multiplicity for the complementary fission fragment ranges.

Mass number interval	$A_L(73-106)$ $A_H(146-179)$	$A_L(106-112)$ $A_H(140-146)$	$A_L(112-126)$ $A_H(126-140)$	$A_L(73-126)$ $A_H(126-179)$
r_{xy}	-0.633373	-0.993743	-0.940186	-0.883037

<center>**CHAPTER 5**</center>

<center>**EXCITATITION ENERGY OF FISSION FRAGMENTS AND ITS PARTITATION BETWEEN THE FISSION FRAGMENTS IN SPONTANEOUS FISSION OF ^{252}Cf**</center>

Model analyses of partitation of fission energy and total excitation energy in fission has been investigated in many works (see for example, [27,14]). General expression for energy release related with different energy kinds in TSM is presented in Introduction. However, in our investigation we shall use experimental data in order to establish excitation energies of individual fission fragments.

Below we introduce some useful expressions for calculation of fission fragment excitation energies by use of experimental data available in litrature.

5.1. General expressions for the excitation energy

Energy release in fission of the given mode is

$$Q = TKE + TEX \tag{5.1.1}$$

where TKE is the total kinetic energy of fission fragments, TEX is the total excitation energy of fission fragments, both of these quantities depend on the mass and charge of complementary fragments, as a form

$$TKE = TKE(Z_1A_1; Z_2A_2), \ TEX = TEX(Z_1A_1; Z_2A_2) \tag{5.1.2}$$

such that, $Z_1 + Z_2 = 92$, $A_1 + A_2 = 252$, where Z_1, Z_2 and A_1, A_2 are the charge and mass numbers of complementary fission fragments, respectively.

The mean excitation energy of each fission fragment may be expressed as dependent on mass number and TKE through by relation given in works [27] and [19] as,

$$\bar{E}_x = \bar{v}(A, TKE) \cdot \bar{E}(A) + \bar{E}_\gamma(A, TKE) \tag{5.1.3}$$

where $\bar{v}(A, TKE)$ is the average number of neutrons (or neutron multiplicity) dependent on mass and TKE, $\bar{E}(A)$ is the average energy carried away per neutron, and has form

$$\bar{E}(A) = B_n(A) + \bar{\varepsilon}(A) \tag{5.1.4}$$

where B_n is the neutron binding energy, and $\bar{\varepsilon}$ is the neutron mean emission energy in the center of mass system of fission fragment. Mean total energy of the γ- rays emitted from fission fragment of given mass A may be calculated by use of Terrell approximation (Ref. [19])

$$\bar{E}_\gamma(A) \cong \frac{\bar{B}_n(A)}{2} \tag{5.1.5}$$

Another expression for mean energy of gamma rays is given by, [26,27]

$$\bar{E}_\gamma(A, TKE) = (0,75 . \bar{v}(A, TKE) + 2)MeV \tag{5.1.6}$$

The formulas from (5.1.3) to (5.1.6) may be written in the forms averaged on TKE of given fission type and written as

$$\bar{E}_x = \bar{v}(A) \cdot \bar{E}(A) + \bar{E}_\gamma(A) = \bar{v}(A) \cdot \left(B_n(A) + \bar{\varepsilon}(A)\right) + \bar{E}_\gamma(A) \tag{5.1.7}$$

In our estimation of fission fragment excitation energy we shall use equation (5.1.7).

For the estimation of $\bar{E}_\gamma(A)$ the relation given in Ref [27] has a form $\bar{E}_\gamma =$

$$\left(6,6867 - 0,15578 \frac{Z_{fn}^2}{A_{fn}}\right) \cdot \bar{v}(A) + \left(0,11127 \frac{Z_{fn}^2}{A_{fn}} - 2,2408\right) MeV \tag{5.1.8}$$

Note that this equation for the average energy of gamma rays doesn't depend on fission fragment mass, but depends on fissioning nucleus charge and mass numbers Z_{fn}, A_{fn}. For estimation $\bar{E}_\gamma$ we shall use the Eq. (5.1.7) which gives dependence on atomic number.

We first investigate neutron average multiplicity included into the Eq. (5.1.7).

5.2   Average energy of emitted neutrons dependent on fission fragment mass

To calculate average excitation energy of fission fragment we need average energy of emitted neutrons dependent on fission fragment mass (see, Eq. (5.1.7)). Below in the Figure 5.1 we illustrate experimental data for neutron average energy dependent on fission fragment mass, taken from Ref.[16].
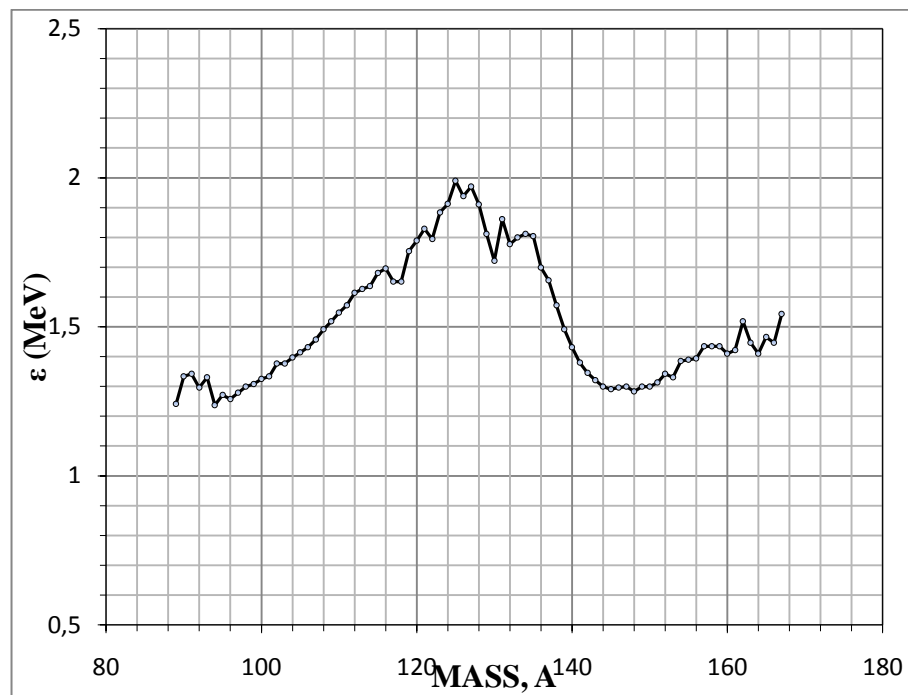
Figure 5.1. Average neutron energy versus fission fragments mass in spontaneous fission of [252]Cf from experiment of Ref.[16]

Using experimental data for average neutron energy we can calculate fission fragments excitation energy by use of values $B_n, \overline{E}_\gamma, \overline{\nu}$.

5.3 Binding energy of neutron for fission fragment of mass number A.

To calculate average excitation energy of fission fragments we first calculate neutron binding energy and average gamma energy for a fission fragment.

For any fission fragment of mass number A, we can calculate neutron binding energy by use of mass table of Ref.[32]. For the different mass and charge numbers from equation

$$B_n(Z, N) = [M(Z, N-1) + M_n - M(Z, N)]c^2, \qquad (5.3.1.)$$

or

$$B_n(Z, A) = [M(Z, A-1) + M_n - M(Z, A)]c^2, \qquad (5.3.2)$$

where $M(Z, N)$ is the atomic mass of nucleus of charge Z and mass number A, taken from Ref[32] , A=Z+N, M_n is the mass of neutron (1.008654u), c is the speed of light. To use one of two last equations we must know the charge number Z that should be integer number. According to Ref [17] the most probable charge values for heavy and light fission fragments in spontaneous fission of ^{252}Cf may be calculated by use of relations

$$Z^p(L) = Z_0 + 0,37 \qquad (5.3.3)$$
$$Z^p(H) = Z_0 - 0,37 \qquad (5.3.4)$$

where $Z_0 = \frac{Z_{fis}}{A_{fis}} \cdot A$ is a charge value in the uniform charge distribution (UCD) model, A is the fission fragments mass, where Z_{fis}, A_{fis} are the charge and mass numbers of fissioning nucleus. For the ^{252}Cf spontaneous fission

$$Z_0 = \frac{98}{252} \cdot A = 0,3889 \cdot A \qquad (5.3.5)$$

5.3.1 Examples of calculating of neutron binding energies for two complementary fission fragments

One can calculate neutron binding energies for fission fragments of mass numbers A = 73, and A=179. For A=73, the charge number in the uniform charge distribution (UCD) model is $Z_0 = \frac{98}{252} \cdot 73 = 28.38$. Using Eq.(5.3.3), find $Z^p(L) =$

28.75, near of 29, so, $Z^p = 29$. So for corresponding nucleus with A=73, Z=29 (^{73}Cu) calculate neutron binding energy by use of mass table in Ref [32], as

$$B_n(Z, A) = [71.9358203 + 1.008654 - 72.936675]c^2$$
$$= 0.0077993 * 931.5 \frac{MeV}{c^2} \cdot c^2 = 7.265 \, MeV$$

For A=179, the charge number in the uniform charge distribution (UCD) model is $Z_0 = 0{,}3889 \cdot 179 = 69.61$. The most probable charge number for the heavy fragment is (Eq.5.3.3) $Z^p(H) = 69.61 - 0{,}37 = 69$ (so,$Z^p = 69$). Now for A=179, Z=69 (^{179}Tm) we find

$$B_n(Z, A) = [177.952640 + 1.008654 - 178.955340]c^2$$
$$= 0.005954 * 931.5 \frac{MeV}{c^2} \cdot c^2 = 5.546 \, MeV$$

Calculation results of binding energy for all fission fragments are shown in the table below.

Table 5.1. Calculated binding energies of neutrons dependent on fission fragment mass number for most probable charges in spontaneous fission of ^{252}Cf.

Mass number (A)	Charge number in (UCD) model (Z_0)	Most probable charge (Z^p)	Binding energy of neutrons (MeV)
73	28,38	29	7,265
74	28,77	29	5,080
75	29,16	30	4,819
76	29,55	30	7,735
77	29,94	30	4,642
78	30,33	31	5,775

79	30,72	31	6.865
80	31,11	31	4,679
81	31,49	32	4,683
82	31,88	32	7,381
83	32,27	33	7,614
84	32,66	33	4,260
85	33,05	33	5,303
86	33,44	34	6,177
87	33,83	34	4,104
88	34,22	35	4,932
89	34,61	35	5,868
90	34,99	35	4,111
91	35,38	36	4,378
92	35,77	36	5,540
93	36,16	37	5,906
94	36,55	37	3,997
95	36,94	37	5,361
96	37,33	38	5,883
97	37,72	38	3,910
98	38,11	38	5,918
99	38,49	39	5,794
100	38,88	39	5,151
101	39,27	40	4,912
102	39,66	40	6,347
103	40,05	40	4,689
104	40,44	41	4,968

105	40,83	41	6,682
106	41,22	42	6,974
107	41,61	42	4,751
108	41,99	42	6,421
109	42,38	43	6,645
110	42,77	43	4,484
111	43,16	44	4,745
112	43,55	44	6,878
113	43,94	44	4,782
114	44,33	45	5,005
115	44,72	45	6,645
116	45,11	45	4,586
117	45,49	46	4,633
118	45,88	46	6,999
119	46,27	47	7,045
120	46,66	47	5,154
121	47,05	47	7,073
122	47,44	48	7,735
123	47,83	48	4,642
124	48,22	49	5,507
125	48,61	49	7,669
126	48,99	49	5,397
127	49,38	49	7,232
128	49,77	49	4,434
129	50,16	50	5,319
130	50,55	50	7,607

131	50,94	51	7,757
132	51,33	51	5,746
133	51,72	51	7,329
134	52,11	52	7,675
135	52,49	52	3,328
136	52,88	52	4,661
137	53,27	53	5,060
138	53,66	53	3,889
139	54,05	54	3,549
140	54,44	54	5,409
141	54,83	54	3,394
142	55,22	55	4,099
143	55,61	55	5,217
144	55,99	56	5,894
145	56,38	56	3,701
146	56,77	56	5,648
147	57,16	57	5,779
148	57,55	57	4,344
149	57,94	58	4,363
150	58,33	58	6,188
151	58,72	58	4,735
152	59,11	59	5,098
153	59,49	59	5,881
154	59,88	60	6,401
155	60,27	60	4,847
156	60,66	60	6,114

157	61,05	61	6,216
158	61,44	61	4,782
159	61,83	61	5,816
160	62,22	62	6,263
161	62,61	62	4,623
162	62,99	63	4,931
163	63,38	63	6,039
164	63,77	63	4,540
165	64,16	64	4,782
166	64,55	64	5,993
167	64,94	65	6,142
168	65,33	65	4,717
169	65,72	65	5,657
170	66,11	66	6,123
171	66,49	66	4,512
172	66,88	66	5,676
173	67,27	67	5,760
174	67,66	67	4,465
175	68,05	68	4,763
176	68,44	68	5,909
177	68,83	68	4,363
178	69,22	69	4,707
179	69,61	69	5,546

Table 5.2. Neutron average energy dependent on fission fragment mass number from experimental work of Ref[16]

Mass number (A)	Average energy of neutrons(MeV)	Mass number (A)	Average energy of neutrons(MeV)
89	1.241	127	1.970
90	1.333	128	1.910
91	1.342	129	1.812
92	1.296	130	1.721
93	1.330	131	1.861
94	1.237	132	1.777
95	1.271	133	1.800
96	1.257	134	1.812
97	1.279	135	1.804
98	1.299	136	1.699
99	1.308	137	1.656
100	1.325	138	1.572
101	1.333	139	1.491
102	1.377	140	1.431
103	1.377	141	1.380
104	1.397	142	1.345
105	1.414	143	1.321
106	1.431	144	1.299
107	1.457	145	1.291
108	1.491	146	1.229
109	1.518	147	1.299
110	1.547	148	1.283

111	1.572	149	1.299
112	1.614	150	1.299
113	1.627	151	1.313
114	1.636	152	1.342
115	1.681	153	1.330
116	1.696	154	1.385
117	1.652	155	1.389
118	1.652	156	1.394
119	1.753	157	1.434
120	1.789	158	1.434
121	1.829	159	1.434
122	1.794	160	1.410
123	1.884	161	1.422
124	1.913	162	1.518
125	1.990	163	1.446
126	1.938	164	1.410
165	1.466	167	1.543
166	1.446		

5.4. Average gamma energy for a fission fragment of mass number A.

To calculate the average gamma energy for a fission fragment of mass number A, we have two formulas, first is approximate Eq.(5.1.5) and second is the Eq.(5.1.7) that is more exact expression. For ^{252}Cf fission fragments we have

$$\bar{E}_\gamma = 1.99982 + 0.749751 \, \bar{v}(A) \qquad (5.\acute{1}.7)$$

The prompt gamma ray energy spectrum of fission fragments in spontaneous fission of ^{252}Cf is broadly discussed in the works [35] and [36]. The results of this works are in correspondence with the Eq.(5.1.7).

Our calculation of average gamma energies are illustrated in Table 5.3 and in the Figures 5.2 and 5.3. Results shown in the figure 5.2 has sawtooth character and is due to binding energy change fron nucleus to nucleus that includes even- odd effect. Figure 5.3 illustrate same character of behaviore versus mass number as for neutron multiplicity.

Table 5.3. Calculated average energies of gamma rays from fission fragments

Fragment Mass Number,(A)	$\overline{E_\gamma} \cong \frac{B_n}{2}$ (MeV) Eq.(5.1.5)	$\overline{E_\gamma}.$ (MeV) Eq(5.1.8)	Fragment Mass Number,(A)	$\overline{E_\gamma} \cong \frac{B_n}{2}$ (MeV) Eq.(5.1.5)	$\overline{E_\gamma}.$ (MeV) Eq(5.1.8)
73	3,632	3,079	111	2,372	3,694
74	2,54	2,839	112	3,439	3,769
75	2,409	2,644	113	2,391	3,889
76	3,867	4,024	114	2,502	3,979
77	2,321	3,529	115	3,322	4,069
78	2,887	2,412	116	2,293	4,159
79	3,432	2,314	117	2,316	4,237
80	2,339	2,224	118	3,499	4,324
81	2,421	2,254	119	3,522	4,414
82	3,679	2,089	120	2,577	4,467
83	3,807	2,104	121	2,572	4,548
84	2,095	2,194	122	3,867	4,616
85	2,608	2,209	123	2,321	4,500
86	3,073	2,344	124	2,753	4,291
87	2,052	2,349	125	3,834	3,949
88	2,421	2,382	126	2,698	3,360

89	2,934	2,465	127	3,616	2,779
90	2,055	2,532	128	2,717	2,569
91	2,189	2,610	129	2,659	2,359
92	2,77	2,695	130	3,803	2,329
93	2,953	2,742	131	3,878	2,389
94	1,998	2,779	132	2,87	2,479
95	2,680	2,787	133	3,66	2,587
96	2,941	2,809	134	3,835	2,674
97	1,955	2,824	135	1,664	2,802
98	2,959	2,872	136	1,887	2,959
99	2,897	2,859	137	2,53	3,004
100	2,575	2,899	138	1,94	3,075
101	2,456	2,914	139	1,773	3,124
102	3,173	2,959	140	2,704	3,154
103	2,344	3,004	141	1,697	3,199
104	2,484	3,064	142	2,049	3,229
105	3,341	3,139	143	2,608	3,259
106	3,487	3,221	144	2,947	3,304
107	2,375	3,311	145	1,850	3,379
108	3,210	3,409	146	2,824	3,414
109	3,322	3,535	147	2,889	3,454
110	2,242	3,614	148	2,172	3,499
149	2,181	3,559	165	2,391	4,249
150	3,094	3,589	166	2,996	4,369
151	2,367	3,649	167	3,071	4,474
152	2,549	3,668	168	2,358	4,29

153	2,940	3,701	169	2,828	4,511
154	3,200	3,761	170	3,061	4,743
155	2,423	3,799	171	2,256	4,998
156	3,057	3,844	172	2,838	4,848
157	3,108	3,859	173	2,88	5,186
158	2,391	3,911	174	2,232	4,414
159	2,908	3,971	175	2,381	4,923
160	3,131	3,971	176	2,954	3,244
161	2,311	4,009	177	2,181	3,311
162	2,465	4,151	178	2,353	2,959
163	3,019	4,200	179	2,773	3,424
164	2,27	4,219			

Table 5.3 data for average gamma energies calculated by use of two formulas are presented in the Figures 5.2 and 5.3. As it seen in Figure 5.2 average gamma energies are changed sharply from fragment to fragment that is due to even-odd struggling effect.
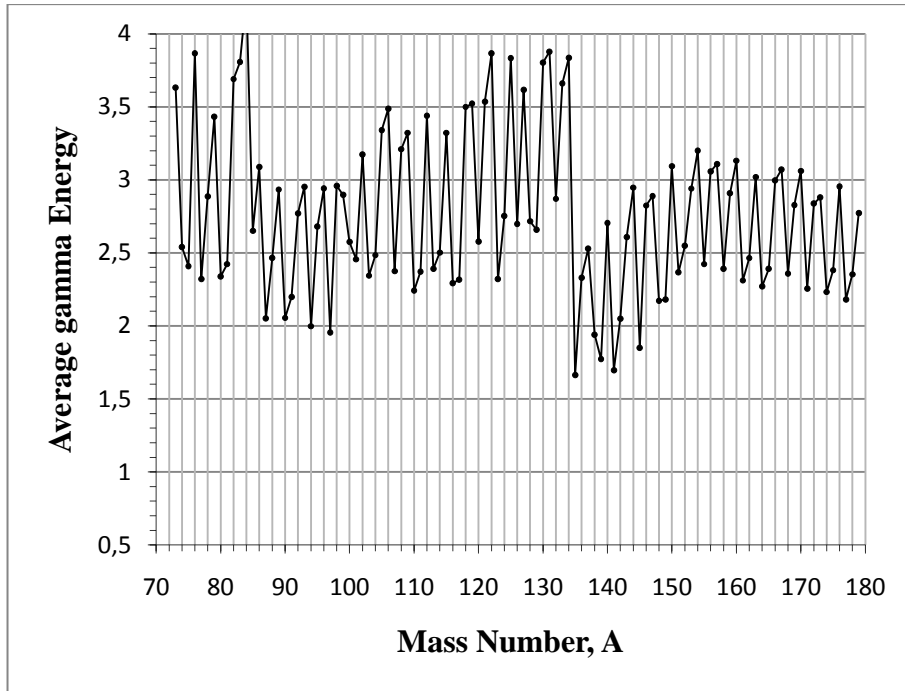
Figure 5.2. Average energies of gamma radiations from fission fragments calculated by approximate relation Eq.(5.1.5).
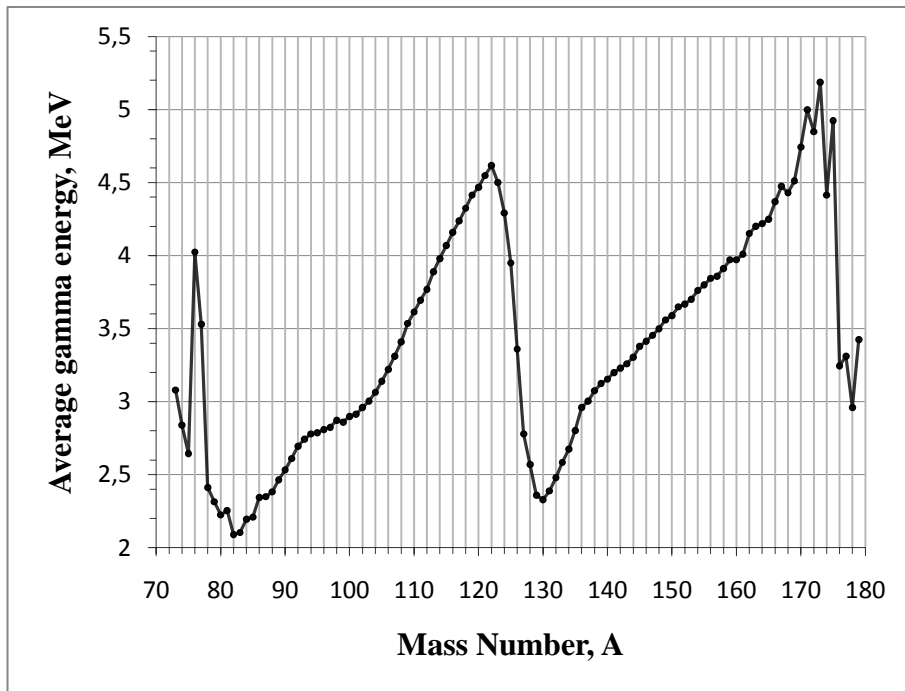

Figure 5.3. Average energies of gamma radiations from fission fragments calculated by Eq.(5.1.8)

5.5 Calculation of average excitation energy

Average excitation energy now can be calculated according to Eq.(5.1.7) by use of above data for neutron multiplicity $\bar{v}(A)$, average neutron energy $\bar{\varepsilon}(A)$, neutron binding energy $B_n(A)$, and average gamma energy $\bar{E}_\gamma(A)$.

Table 5.4. Average excitation energy of fission fragments .

Fragments mass number, A	Excitation energy, MeV Eq.(5.1.7) and Eq.(5.1.5)	Excitation energy, MeV Eq.(5.1.7) and Eq.(5.1.8)	Fragments mass number, A	Excitation energy, MeV Eq.(5.1.7) and Eq.(5.1.5)	Excitation energy, MeV Eq.(5.1.7) and Eq.(5.1.8)
89	7.384	6.879	127	13.186	12.349
90	5.920	6.397	128	8.298	8.150
91	6.845	7.266	129	6.081	5.781
92	9.113	9.038	130	7.907	6.433
93	10.116	9.905	131	8.879	7.390
94	7.441	8.222	132	7.680	7.289
95	9.643	9.750	133	10.773	9.697
96	10.652	10.520	134	12.368	11.207
97	7.662	8.531	135	7.155	8.293
98	11.359	11.272	136	10.470	9,962
99	11.042	11.004	137	11,529	12.003
100	10.346	10.670	138	7.255	8.390
101	10.074	10.532	139	9.333	10.684
102	13.059	12.845	140	13.237	13.687
103	10.472	11.132	141	9.335	10.837
104	11.522	12.102	142	10.977	12.157
105	15.646	15.444	143	13.591	14.242
106	17.187	16.921	144	15.462	15.819

|					
107	13.294	14.230	145	11.035	12.564
108	18.084	18.283	146	15.927	16.517
109	19.937	20.252	147	16.620	17.185
110	15.226	16.598	148	13.426	14.753
111	19.648	17.970	149	13.957	15.335
112	23.480	23.810	150	18.966	19.461
113	18.541	20.039	151	15.672	16.954
114	20.034	21.511	152	14.884	18.003
115	26.301	27.048	153	19.308	18.069
116	20.388	22.254	154	20.601	21.162
117	21.076	22.997	155	17.389	18.765
118	30.317	31.142	156	21.526	22.313
119	32.851	32.743	157	22.080	22,813
120	25.426	27.316	158	18.241	19.761
121	33.802	28.259	159	21.975	23.038
122	37.123	37.872	160	23.310	24.150
123	24.085	26.264	161	18.511	20.209
124	25.428	26.966	162	20.973	22.659
125	28.947	29.062	163	24.987	26.168
126	16.011	16.673	164	19.882	21.831
165	21.135	22.993	167	28.431	32.905
166	29.503	27.876			
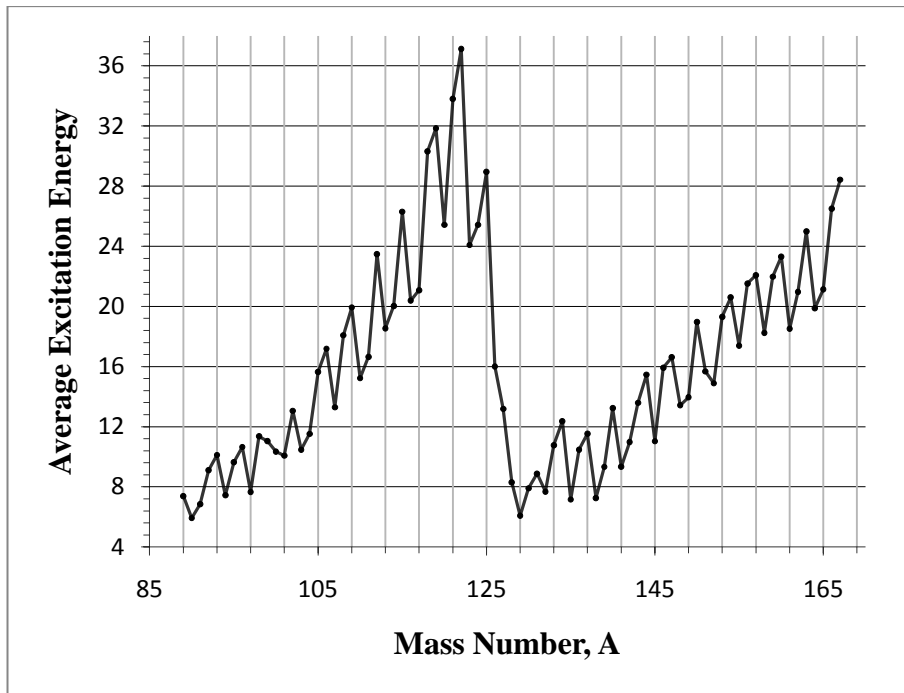
Figure 5.4. Average excitation energy of fission fragments calculated from general expression Eq.(5.1.7) by use of Eq.(5.1.5) for average gamma energy.
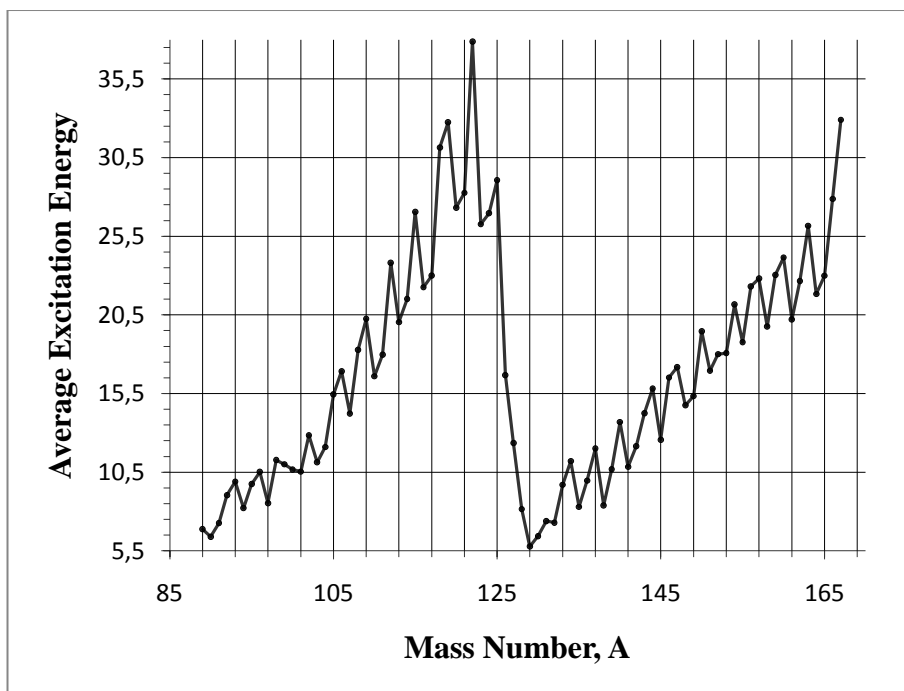
Figure 5.5. Average excitation energy of fission fragments calculated from general expression Eq.(5.1.7) by use of Eq.(5.1.8) for average gamma energy.

Below in the figures 5.6-5.13 are illustrated correlation of excitation energies from complementary fission fragments in the different light and complementary heavy fragment mass ranges for two methods of calculations discussed above in the text.
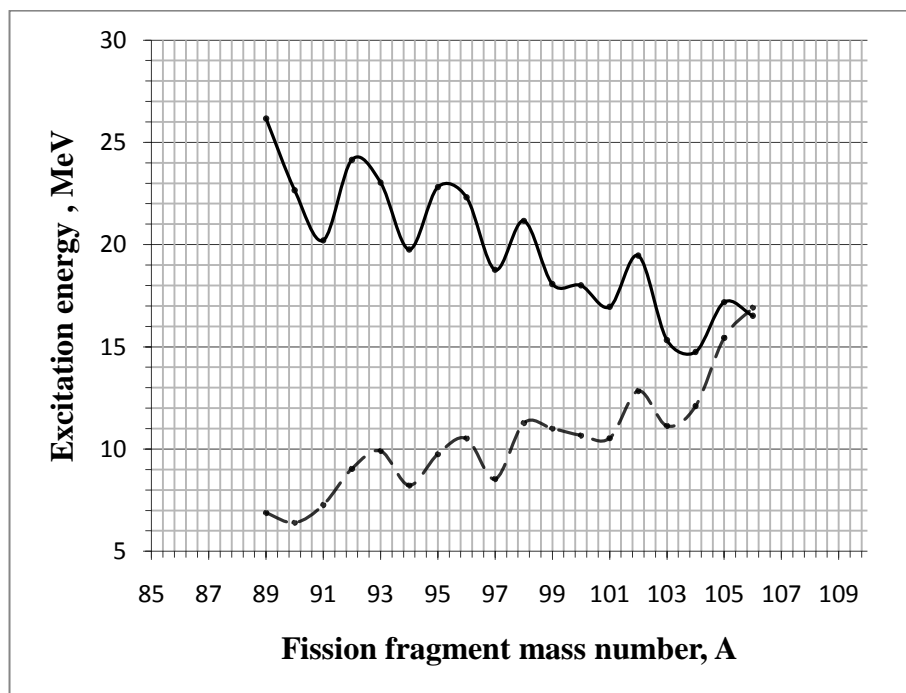

Figure 5.6. Fission fragments excitation energies in the light fragment mass range(89 − 106),(dashed curve), and complementary heavy fragment mass range(146 − 167) (solid curve) by use of Eqs.(5.1.7),(5.1.8)

Figure 5.7. Fission fragments excitation energies in the light fragment mass range$(89 - 106)$,(dashed curve), and complementary heavy fragment mass range$(146 - 167)$ (solid curve) by use of Eqs.(5.1.7),(5.1.5)
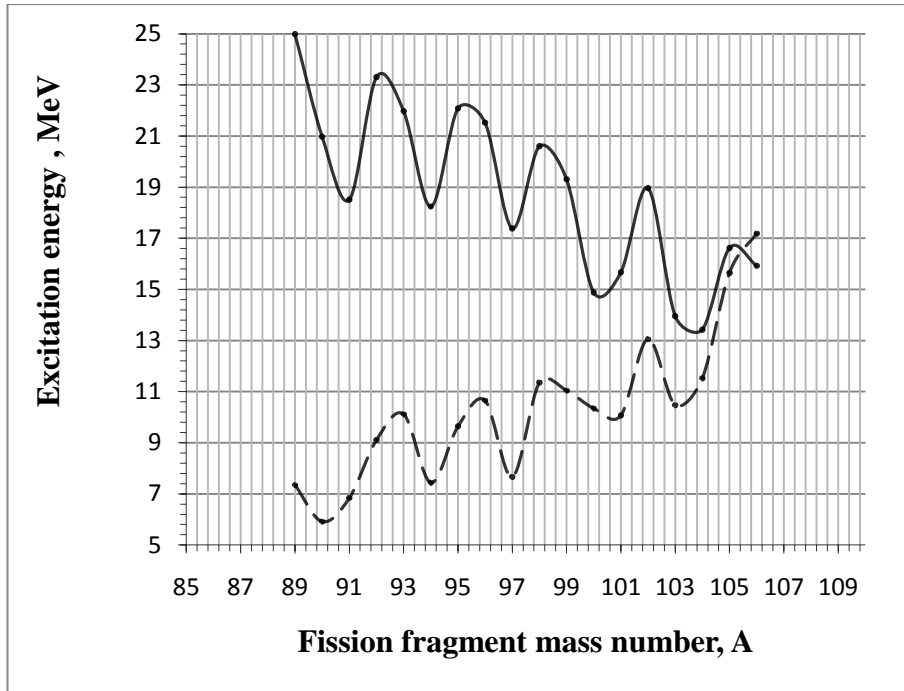
Figure 5.8. Fission fragments excitation energies in the light fragment mass range$(106 - 112)$,(dashed curve), and complementary heavy fragment mass range$(140 - 146)$ (solid curve) by use of Eqs.(5.1.7),(5.1.8)

Figure 5.9. Fission fragments excitation energies in the light fragment mass range$(106 - 112)$,(dashed curve), and complementary heavy fragment mass range$(140 - 146)$ (solid curve) by use of Eqs. (5.1.7),(5.1.5)

Figure 5.10. Fission fragments excitation energies in the light fragment mass range$(112 - 126)$,(dashed curve), and complementary heavy fragment mass range$(126 - 140)$ (solid curve) by use of Eqs. (5.1.7),(5.1.8)
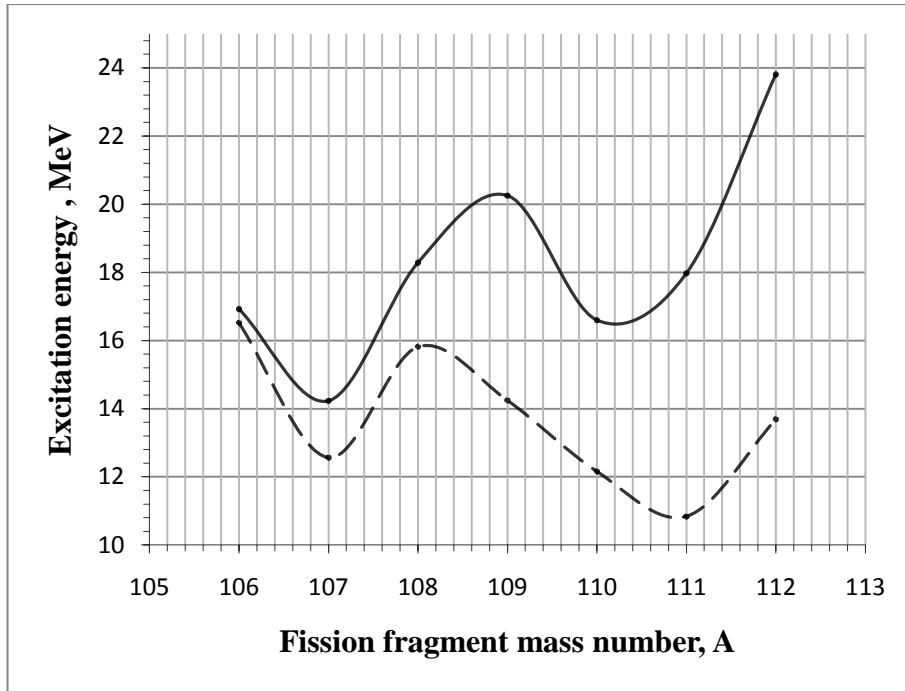
Figure 5.11. Fission fragments excitation energies in the light fragment mass range(112 − 126),(dashed curve), and complementary heavy fragment mass range(126 − 140)(solid curve) by use of Eqs. (5.1.7),(5.1.5)
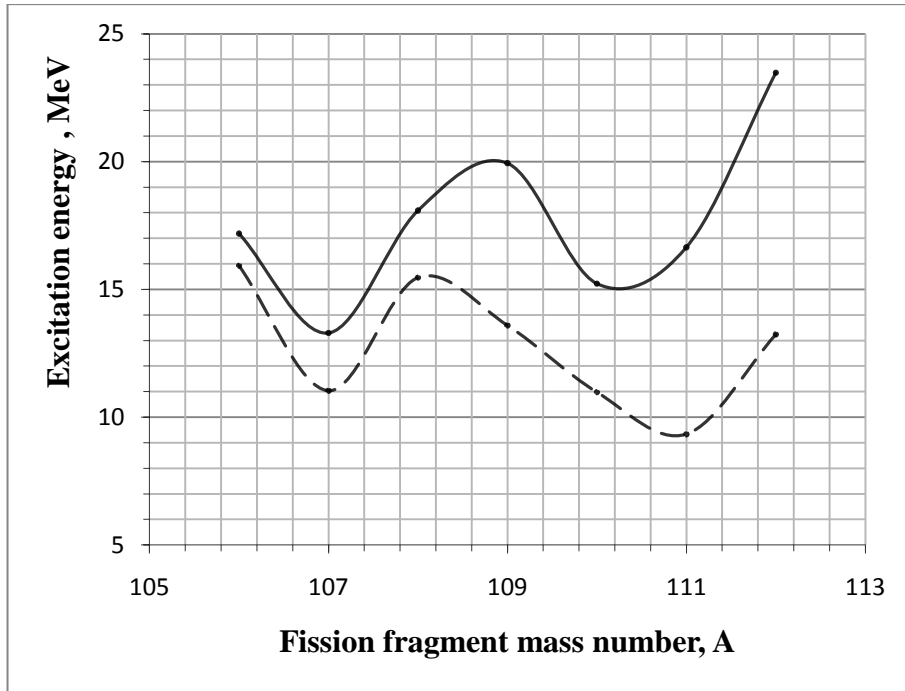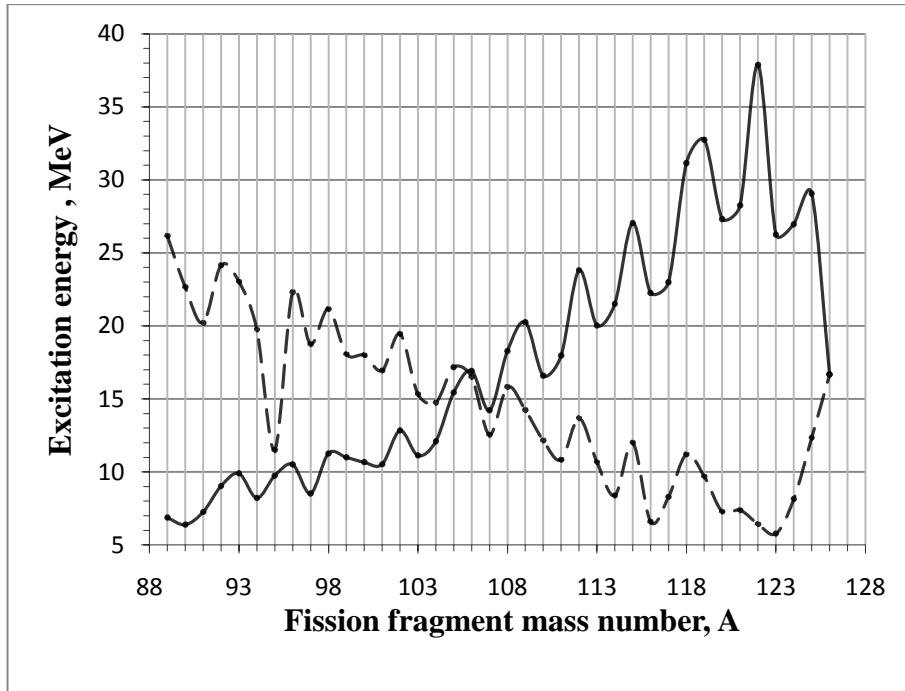
Figure 5.12. Fission fragments excitation energies in the light fragment mass range$(89 - 126)$,(dashed curve), and complementary heavy fragment mass range$(126 - 167)$ (solid curve) by use of Eqs. (5.1.7),(5.1.8)
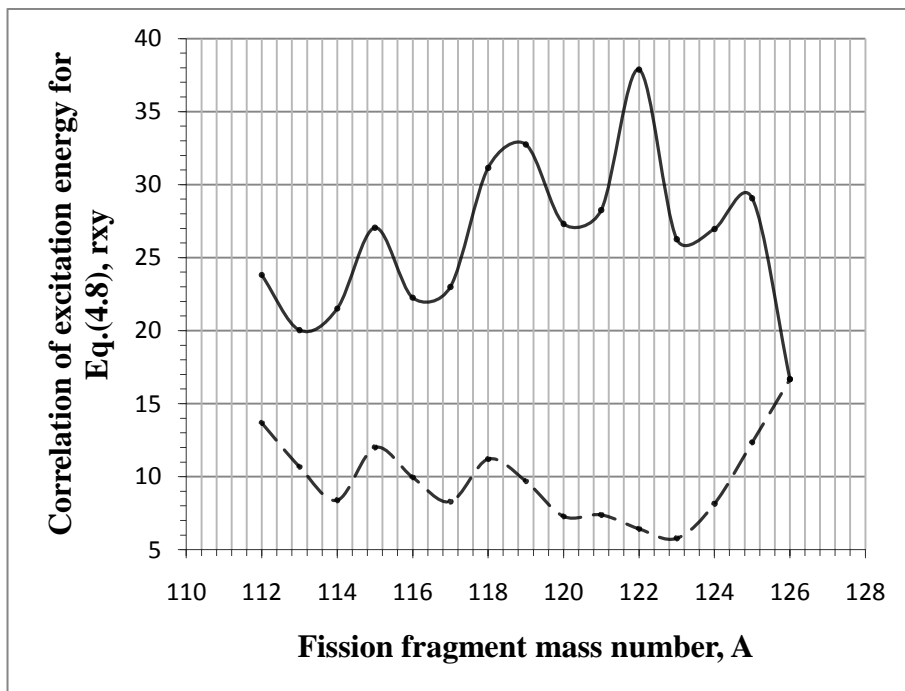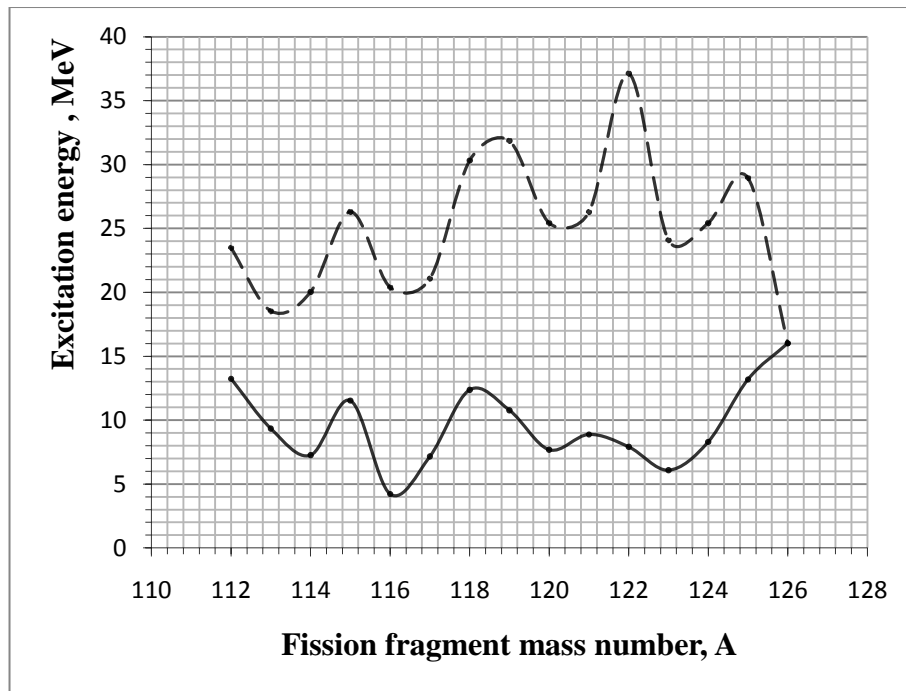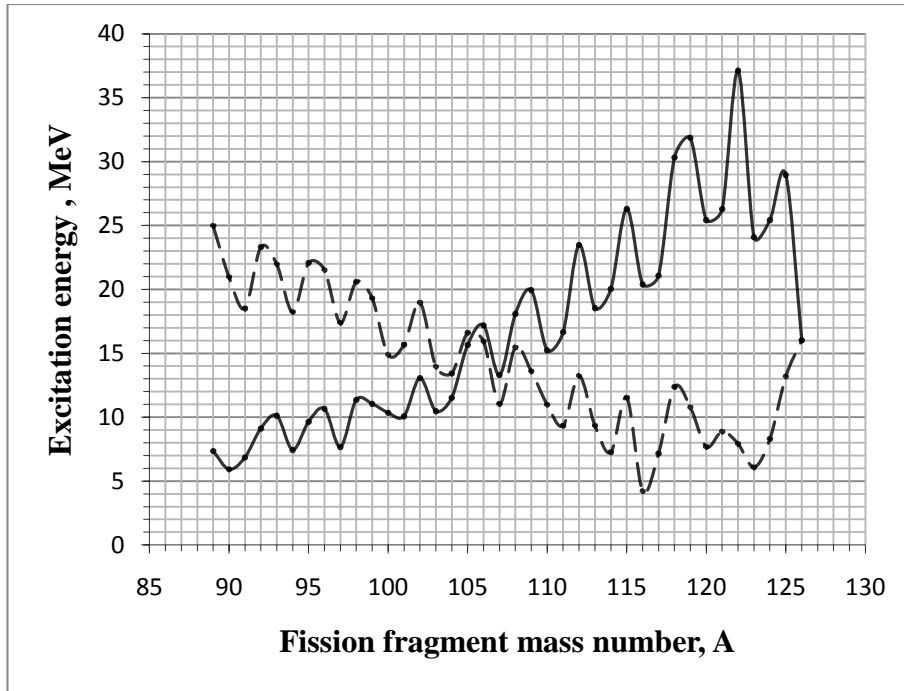
Figure 5.13. Fission fragments excitation energies in the light fragment mass range$(89 - 126)$,(dashed curve), and complementary heavy fragment mass range$(126 - 167)$ (solid curve) by use of Eqs.(5.1.7),(5.1.5)

Table 5.5. Pearson correlation coefficient (r_{xy}) of excitation energy for the complementary fission fragment ranges.

Mass number, A	$A_l(89 - 106)$ $A_h(14 - 163)$	$A_l(106 - 112)$ $A_h(140 - 146)$	$A_l(112 - 126)$ $A_h(126 - 140)$	$A_l(89 - 126)$ $A_h(126 - 163)$
Excitation energy for Eq.(5.1.8)	−0.606669	0.142204	−0.462254	−0.855194
Excitation energy for Eq.(5.1.5)	−0.390224	0.188467	−0.135161	−0.741780

5.6. Calculation of the total excitation energy

To compaire our result with experimental data of work [37] we calculate total excitation energy of complamentary fission fragments fron relation

$$\overline{E_X^{tot}} = \overline{E_X}(A_L) + \overline{E_X}(A_H) \qquad (5.6.1)$$

In table 5.6 are listed results of calculation.

Table 5.6. Table of total excitation energy

Mass Number, A	Total Excitation Energy Eqs.(5.1.7), (5.1.5) MeV	Total Excitation Energy Eqs.(5.1.7), (5.1.5) MeV	Mass Number, A	Total Excitation Energy Eqs.(5.1.7), (5.1.5) MeV	Total Excitation Energy Eqs.(5.1.7), (5.1.5), MeV
89	33,047	33,047	108	34,102	34,102
90	28,579	28,579	109	34,179	34,179
91	27,054	27,054	110	28,755	28,755
92	33,263	33,263	111	28,807	28,807
93	33,154	33,154	112	37,497	37,497
94	27,283	27,283	113	30,723	30,723
95	32,563	32,563	114	29,901	29,901
96	32,833	32,833	115	39,051	39,051
97	27,296	27,296	116	32,216	32,216
98	32,434	32,434	117	31,129	31,129
99	29,073	29,073	118	41,524	41,524

100	28,673	28,673	119	42,440	42,440
101	27,486	27,486	120	34,605	34,605
102	32,306	32,306	121	36,649	35,649
103	26,467	26,467	122	44,305	44,305
104	26,855	26,855	123	32,045	32,045
105	32,629	32,629	124	35,264	35,264
106	33,438	33,438	125	41,411	41,411
107	26,794	26,794	126	37,346	33,346

Figures 5.14 and 5.15 are illustrate graphs of total excitation energy dependent on light fragment mass.

Note that the results are agrrement with experimental data of work [37] if take into account that experimental results of total excitation energy partitation in 12 MeV proton enduced fission of [232]Th include segnificante symmetric fission mode in addition to asymmetric one.
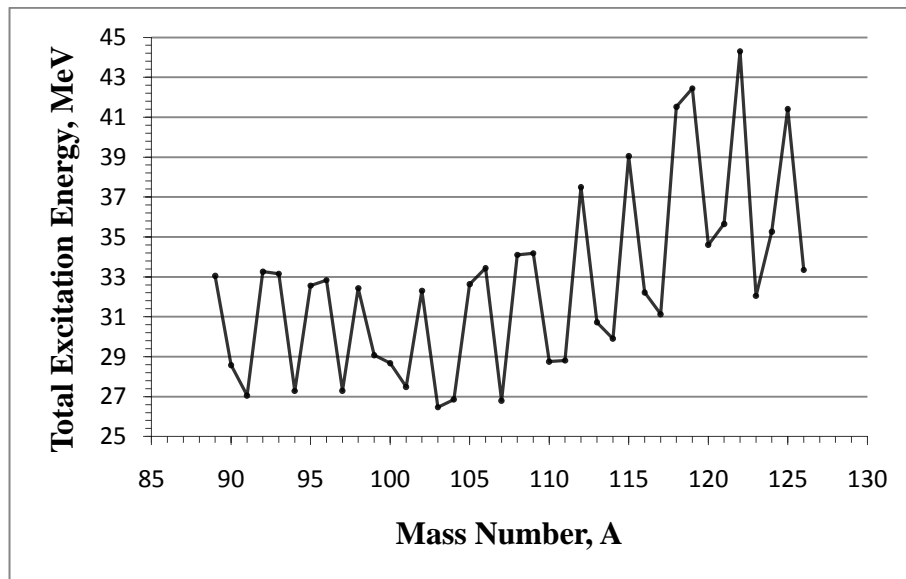

Figure 5.14. Total excitation energy for Eqs.(5.6.1), (5.1.7), (5.1.8)

Total average excitation energy from complementary fission fragments are found to be ~ 30 MeV in the light fragment mass range (89-110), ~ 33 MeV in mass range (110-117), ~ 37 MeV in mass range (117-126). These results are in correspondence with the experimental data on 12 MeV proton induced fission of thorium.
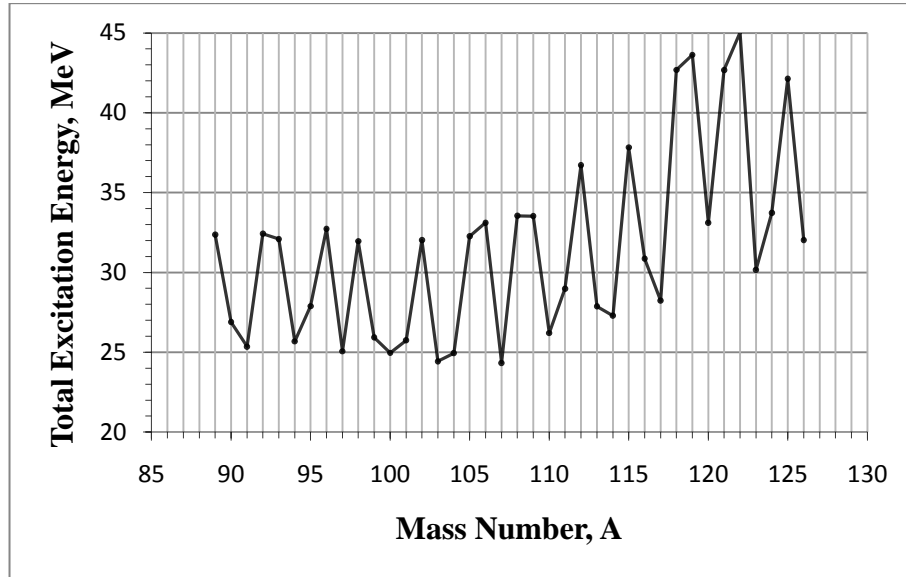
Figure 5.15. Total excitation energy for Eqs.(5.6.1), (5.1.7), (5.1.5)

5.7   Ratio of fragments excitation energy to the total excitation energy

The ratio of fission fragment excitation energy to the total excitation energy of complementary fragments is also used as characteristics of excitation energy partitation between the fission fragments. This ratio has form

$$R = \frac{\overline{E_X(A_L)}}{\overline{E_X^{tot}}} \tag{5.7.1}$$

Table 5.7. Table of the ration of excitation energy to total excitation energy

Mass Number, A	The ratio of $\frac{\overline{E_X}(A_L)}{E_X^{tot}}$ for Eqs.(5.7.1), (5.1.5)	The ratio of $\frac{\overline{E_X}(A_L)}{E_X^{tot}}$ for Eqs.(5.7.1), (5.1.8)
89	0,226	0,208
90	0,220	0,223
91	0,269	0,268
92	0,281	0,271
93	0,315	0,298
94	0,289	0,301
95	0,345	0,299
96	0,325	0,320
97	0,305	0,312
98	0,355	0,347
99	0,425	0,378
100	0,414	0,372
101	0,391	0,383
102	0,407	0,397
103	0,428	0,420

104	0,461	0,450
105	0,484	0,473
106	0,519	0,506
107	0,546	0,531
108	0,539	0,536
109	0,594	0,592
110	0,581	0,577
111	0,677	0,623
112	0,639	0,634
113	0,665	0,652
114	0,734	0,719
115	0,695	0,692
116	0,660	0,690
117	0,746	0,738
118	0,710	0,749
119	0,753	0,771
120	0,768	0,789
121	0,615	0,792
122	0,824	0,854
123	0,798	0,819
124	0,753	0,764
125	0,687	0,701

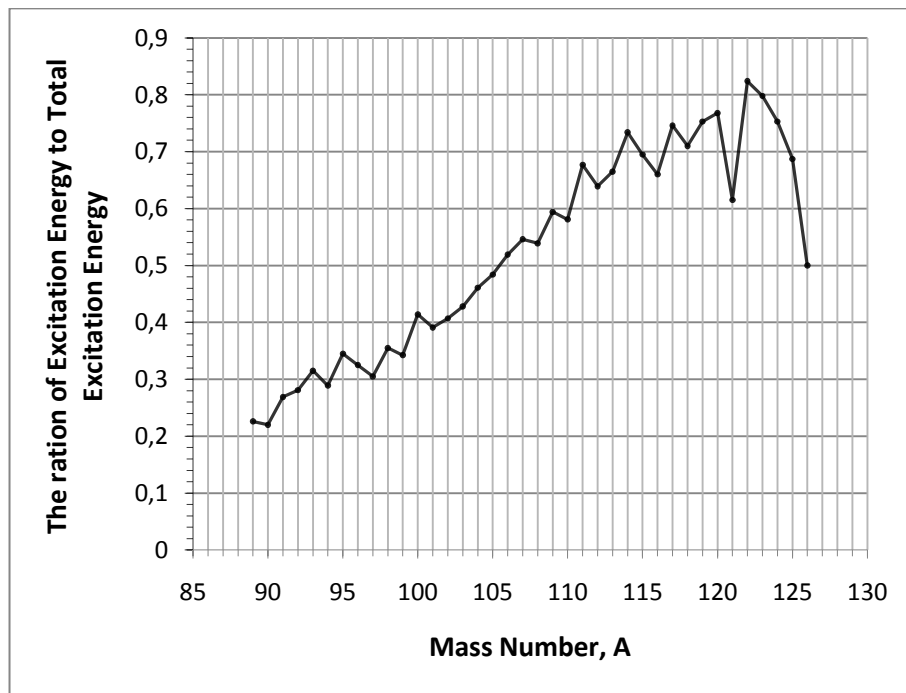| 126	0,500	0,500

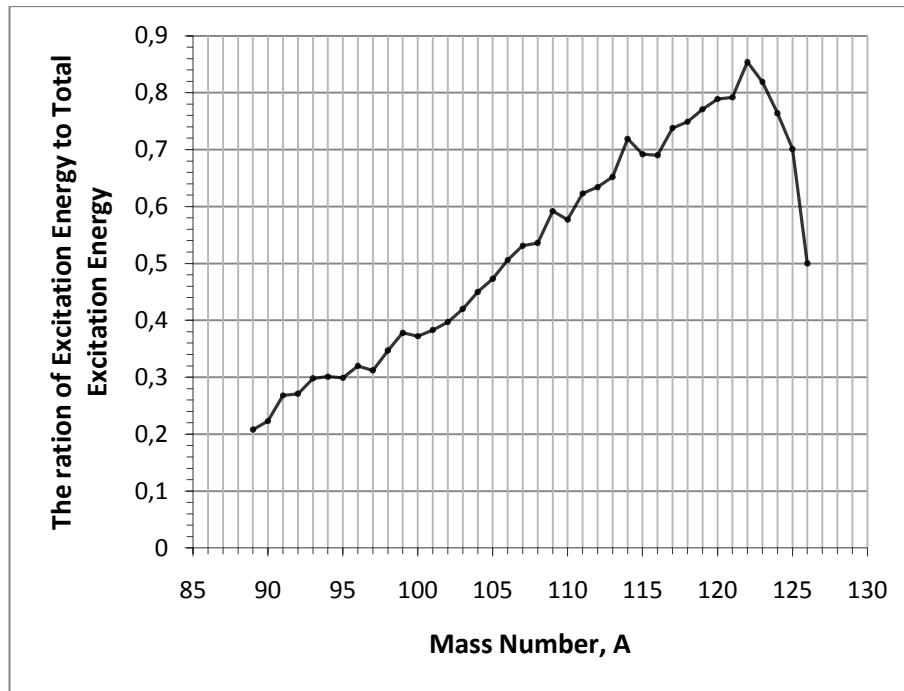Figure 5.16. The ratio of *R* for Eqs.(5.7.1), (5.1.5)

Figure 5.16. The ratio of *R* for Eqs.(5.7.1), (5.1.8)

The ratio of fragment excitation energy to the total excitation energy of fragment pair is monotonically increased from 0,2 at the mass 89 to 0,85 at mass number 122 and then dicreassing to 0,5 at a symmetric mass 126. Slope of this dependence in the mass range 89-122 is equal to 0,019. This result is also coincide with the corresponding experimental result for proton induced fission of [232]Th. For asymmetric mass yield mode it is found in this experiment that the ratio of fragment excitation energy to the total excitation energy has approximately linear dependence with the slope 0,02 in the mass range corresponding to 84-108 where symmetric fission mode contribution is negligible.

RESULTS AND CONCLUSION

The details of work made in thesis in order to calculate fission fragment excitation energies in spontaneous fission of ^{252}Cf may be listed as followings:

1- Fission fragment most probable charges were calculated for fission fragment identification.

2- Neutron binding energy for fission fragments, by use of atomic mass data table AME2003 was calculated in order to estimate average energy of gamma rays emitted from fragments within the Terrell approximation, as well as for calculating of fission fragment excitation energy.

3- Average energy of gamma rays were calculated by use of empirical expression including neutron multiplicity dependent on fragment mass and by use of neutron binding energy in fragment.

4- Experimental data of Budtz – Jorgenson and Knitter for average neutron energy, dependent on fragment mass in graphical representation were used for calculation of fragment excitation energy.

5- Experimental data of Budtz – Jorgenson and Knitter on neutron average multiplicity, dependent on fragment mass in digital form were used for calculation of fragment excitation energy.

6- In order to calculate correlation between neutron multiplicities and average excitation energies of fission fragments, fission fragment mass region is divided into three ranges- (89-106),(163-146); (106-112),(146-140); (112-126),(140-126), where mass yields are monotonicly increasing and deacrising, approximatlly constant, and deacrising and increasing, respectively for complementary fragments.

7- Correlation of neutron multiplicities and fisson fragment excitation energies were calculated in these three mass ranges and in the whole mass range of complementary fragments, (89-126) and (126-163).

8- As a measure of these correlations the Pearson correlation coeficient is calculated in all cases.

9- Totat excitation energy of complementary fission fragments is calculated.

10- The ratio of fission fragment excitation energy to the total excitation energy of fragment pair is calculated.

On a base of analysis made above the following results are found.

There is the strong anticorrelation (with correlation coeeficient r_{xy}= -0,994) between the neutron multiplicities in the mass ranges corresponding to the maximum mass yield range of complementary fragments (106-112); (146-140) where mass yields are approximatlly constant. It is found that there are higher anticorrelation with correlation coeeficient. r_{xy}= -0,940, in the mass ranges of complementary fragments (112-126); (140-126) where mass yields are monotoniclly changed around the symmetric fission mode. In the mass ranges of complementary fragments (73-106); (179-146) anticorrelation of neutron multiplicities is less stronger then in the first two ranges above indicated, namely r_{xy}= -0.633. This result is due to contribution of neutron multiplicities from the masses in the tail of mass distribution. In the whole mass ranges of complementary fission fragments (73-126); (179-126), correlation cooeficient is found to be r_{xy} = -0,883. Characterization of partitation of total excitation energy between the fission fragments through the correlation of excitation energies from complementary fission fragnents shows that a small correlation between the excitation energies (r_{xy}= 0,142) is valid in the mass ranges (106-112); (146-140) corresponding to the maximum mass yield of fission fragments. This result is in correspondence with the litretuer data and has great importance in many applications of neutron physics. A slower anticorrelation between the excitation energies, than between neutron multiplicities, are found, (r_{xy}= -0,607) in the mass ranges (89-106); (163-146), r_{xy}= -0,462 in the mass range (112-126); (140-126), and r_{xy}= -0,855 in the whole mass range (89-126); (163-126). Total average excitation energy from complementary fission fragments are found to be $\sim$ 30 MeV in the light fragment mass range (89-110), $\sim$ 33 MeV in mass range (110-117), $\sim$ 37 MeV in mass range (117-126). These results are in correspondence with the experimental data on 12 MeV proton induced fission of thorium. The ratio of fragment excitation energy to the total excitation energy of fragment pair is monotonically increased from 0,2 at the mass 89 to 0,85 at mass number 122 and then dicreassing to 0,5 at a symmetric mass 126. Slope of this dependence in the mass range 89-122 is equal to 0,019. This result is also coincide with the corresponding experimental result for proton induced fission of [232]Th. For the

asymmetric mass yield mode it is found in this experiment that the ratio of fragment excitation energy to the total excitation energy has approximately linear dependence with the slope 0,02 in the mass range corresponding to 84-108 where symmetric fission mode contribution is negligible.

This result indicate that energy partition mechanisms for spontaneous fission of ^{252}Cf and induced fission of ^{232}Th are similar at least, for the asymmetric fission mode of this nucleus.

REFERENCES

[1]   Amaldi, E., D'Agostino, O., Pontecorvo, B., Fermi, E.,Rasetti, F., Segre, E. (1935).Aritificial radioactivity produced by neutron bombardment II, *Proc. Roy.Soc. Lond,* **A149***,* 522-558.

[2]   Meitner, L., Hahn, O. (1936). Neue umwandlungsprozesse bei bestrahlung des urans mit neutronen, *Naturwissenschaften* , **24**,158-159.

[3]   Meitner, L.(1936). Kunstlicke umwandlungsprozesse beim uran, *Kernphysik*, **S**, 24-42.

[4]   Meitner, L., Hahn, O., Stressmann, F. (1937). Uber die umwandlungstreihen des urans, die durch neutronenbest rahlung erzeugz werden, *Z.Physik*, **106**, 249-270.

[5]   Meitner, L., Frish, O.R. (1939). Disintegration of uranium by neutrons: A new type of nuclear reaction, *Nature*, **143**, 239-240.

[6]   Frish, O.R. (1939). Physical evidence for the division of heavy nuclei under neutron bombardment, *Nature*, **143**, 276-276.

[7]   Bohr, N. (1936). Neutron capture and nuclear constitution, *Nature* ,**137,** 344 -348.

[8]   Bohr, N. (1939). Desintegration of heavy nuclei, *Nature*, **143**, 330-331.

[9]   Bohr, N., Wheeler, J.A. (1939). The mechanism of nuclear fission, *Phys.Rev*, **56**, 426-450.

[10]   Marten, H. et al.(1986). Calculation of prompt fission neutron spectra for applied purposes, Proc. IAEA advisory group meeting on properties of neutron sources. Leningrad., IAEA- TECDOC-410, Vienna 153-157.

[11]   Marten, H. Ruben, Seeliger, A. D. (1988). Fission energetiecs and prompt neutron emission, *Physics of Neutron Emission in Fission*, Procceding of Consultant Meeting, IAEA, Mito, Japan, **24-27** May,47-57.

[12]   Terrell, J. (1965). Prompt neutrons from fission, *Physics and Chemistry of Fission* ,Proc. IAEA Symp,Salzburg, Vienna, **II**, 3.

[13]   Marten, H. (1987). Theoretical models and computer programs for the calculation of prompt fission neutron spectrum, Proc. IAEA advisory group meeting on nuclear theory for fast neutron nuclear data evalution, Beijing., IAEA- TECDOC-483, Vienna, 148-159.

[14]   Schmidt, Karl-Heinz ., Jurado, Beatriz. (2011). Final excitation energy of fission fragments, *Physical Review*, **C 83**, 061601(R)

[15]   Gilbert, A., Choen, F. S., Cameron , A. G.W. (1965). Level densities in lighter nuclei, *Can. J. Phys*. **43**, 1248-1255.

[16]   Budtz-Jorgensen C., Knitter K. (1988). Simulaneous investigation of fission fragments and neutrons in ^{252}Cf (SF), *Nuclear Physics*, **A490**, 307-328.

[17]   Unik J.P., Gindler J.E., Gelendenin L.E., Flynn K.F., Gorski A., Sjoblom R.K. (1973). Fragment mass and kinetic energy distributions for fissioning systems ranging from mass 230 to 256, *Proc. IAEA. Symp. Phys. Chem. Fission*, 3rd, Vienna, **II**, 19-45.

[18]   Marten H., Ruben, A., Seeliger, D. (1988). Fission enetrgitiecs and prompt neutron emission, Physics of neutron emission in fission, Proc. IAEA consultant meting on physics of neutron emission in fission, Mito, Japan, 47-57.

[19]   Terrell, J. (1959). Fission neutron spectra and nuclear temperatures, *Phys,Rev*.**113**,527-541.

[20]   Wilkins, B. D., Steinberg, E.P., Chasman, R.R. (1976). Scission- point model of nuclear fission based on deformed-shall effects, *Physical Review C*, **14**, No 5, 1832-1863.

[21] Vandelbosch, R., Huizenga, J. R.. (1973). Nuclear Fission, Acadimic Press, New York and London.

[22] Myers,W.D., Swiatecki, W.J (1966). Nuclear masses and deformations, *Nucl. Phys*, **81**,1-60.

[23] Strutinski, V.M.. (1968). Shells in deformed nuclei, *Nucl. Phys,* **A 122**, 1-33.

[24] Krappe, H.J., Nix, J.R. (1973). *Proc. IAEA. Symp. Phys. Chem. Fission*, 3rd, Vienna, **I**, 159-172.

[25] Bardeen J., Cooper J. L.N., Schreiffer J. (1957). Theory of superconductivity, *Phys.Rev*. **108**,1175-1204.

[26] Nifenecker H., Signarbieaux C, Babinet R. Poiton J. (1973). Neutron and gamma emission in fission, *Proc. IAEA. Symp. Phys. Chem. Fission*, 3rd, Vienna, **II**, 117-179.

[27] Signarbieaux C, Babinet R., Nifenecker H., Poiton J. (1973). Etude experimentale de la correlation entre les numbers de neutrons prompt emis par les deux fragments complementaires dans la fission spontanee de ^{252}Cf, *Proc. IAEA. Symp. Phys. Chem. Fission*, 3rd, Vienna, **II**, 179-189.

[28] Brosa, U., Grossmann, S., Müller, A. (1990). Nuclear scission, *Physics Reports* **197**, 167 – 262.

[29] Hambsh, F. J., Oberstedt, S., van Aarle, J., Barreau, G. (1997). The IRMM experimental data on fission fragment mass distribution, Proceedings of the international conference on fission and proprieties of neutron- rich nuclei, Sanibel Island, Florida, USA. World Scientific, Singapore, 86-95.

[30] Hambsh F. J., Anabella Tudora, Vladuca G., Oberstedt S. (2005). Prompt fission neutron spectrum evaluation for ^{252}Cf in the frame of the multi-modal fission model, *Annals of Nuclear Energy* ,**32**, 1032-1046.

[31] Erten, H.N., Aras, N.K. (1979). Charge distribution in the spontaneous fission of ^{252}Cf, *J.Inorg, Nucl. Chem*, **41,** 149-154.

[32] Audi, G., Wapstra, A.H., Thibault, C. (2003). The ame2003 atomic mass evaluation (II), Tables, graphs and references, *Nuclear Physics*, **A 729** ,337–676.

[33] Deruytter, A.J., Wegner- Penning, G. (1974). Comparison of the fission characterictics of thermal neutron induced fission of [239]Pu and the spontaneous fission of [240]Pu. *Physics and Chmestry of Fission*, **2**, 51-63.

[34] Friedland,S.S. (1951). Energy Distribution of Fission Fragments of U[235]   Produced by 2.5-Mev and 14-Mev Neutrons, Phys. Rev, 84, 75-77.

[35] Verbinski, V., Weber, H., Sund, R. E. (1973). Prompt Gamma Rays from 235U(n,f), 239Pu(n,f) and Spontaneous Fission of [252]Cf, *Phys. Rev,* **C7**, 1173-1185.

[36] Smith, A. B., Fields,P. R., Friedman,A. M. (1956). Prompt Gamma Rays Accompanying the Spontaneous Fission of [252]Cf, *Phys. Rev,* **104**, 699-702.

[37] Nishanaka, I., Nagame, Y., Lkezoe, H., Tanikawa, M., Zhao, Y.L., Sueki, K., Nakahara, H. (2004). Partitation of total excitation energy between fragment pairs in asymmetric and symmetric fission modes, *Phys. Rev,***C70**, 014609-1-10.

[38] Blinov, M.V., Kazarinov, N.M., Krisyuk, I.T., Kovalenko, S.S. (1970). On partitation of excitation energy between fission fragments in termal neutron fission of [235]U *Sov. J, Nucl.Phys,* **10**, 533-541.

[39] Nifenecker, H., Frehau,t J., Soleilhac, M. (1969). Etude de l'emission neutronique des fragments de fission du [252]Cf en fonction de leur charge, *Proc. IAEA. Symp. Phys. Chem. Fission*, 2nd, Vienna, 1969, 491-505.

[40] Bowman, H.R., Milton, J.C.D., Thompson, S.G., Swiatecki, W.J. (1963). Further studies of the prompt neutrons from the spontenatous fission of [252]Cf , *Phys, Rev.* **129**, 2133-2147.

[41] Gavron, A., Fraenkel, Z. (1971). Measurement of the variance of the number of neutrons emitted in fission of [252]Cf as function of the fragment mass and total kinetic energy, *Phys. Rev. Lett*. **27**, 1148-1157.